

# Determining the frequency dependence of elastic properties of fractured rocks

**BENEDIKT AHRENS & JOERG RENNER | 19.04.2016**



## Scaling determines homogeneity!

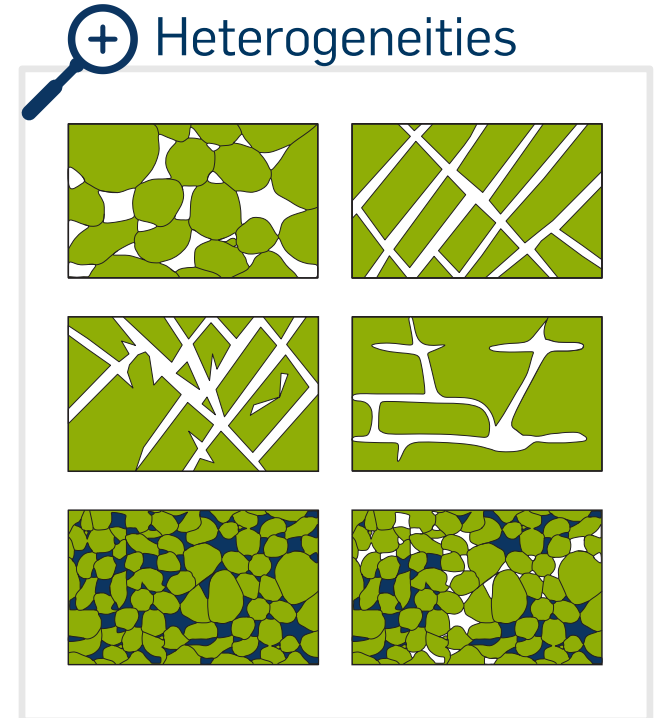
Rocks contain joints or faults on various length scales that have a profound effect on fluid flow, heat transport and elastic properties of rocks.



**Understanding the effect of fractures on elastic properties is important for the characterization of deep geothermal reservoirs.**



Seismic surveys are a valuable tool to investigate fractured rocks but the extraction of fracture properties remains difficult.

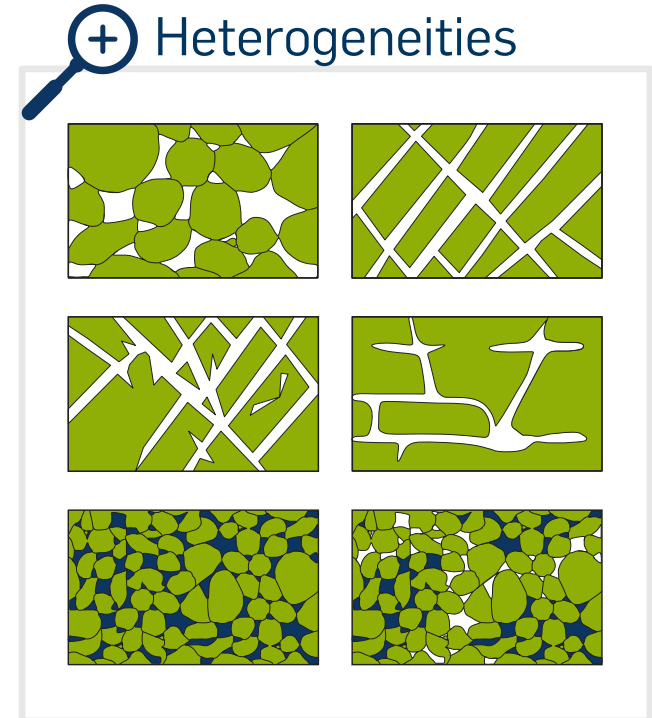


## Scaling determines homogeneity!

Frequency-dependent interaction between fractured rocks and viscous pore fluids require well-founded dispersion analyses.



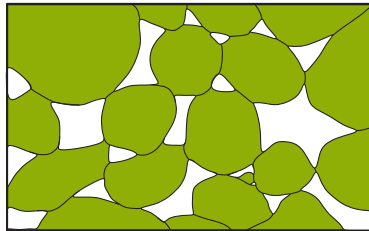
**Experimental investigation of the effective elastic properties of fractured reservoir rocks over relevant frequencies:**



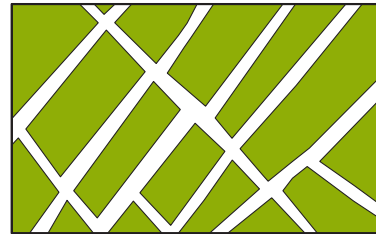
## Scaling determines homogeneity!



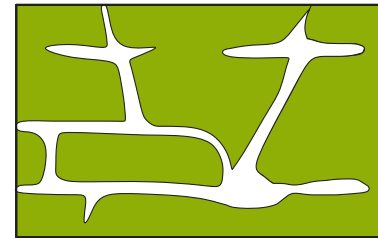
### Rock frame



pores ( $\mu\text{m}$ )



joints (cm...m)

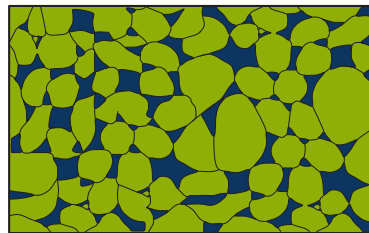


karsts (m)



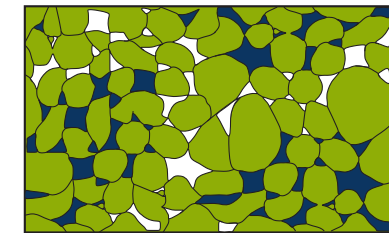
faults ( $\mu\text{m}$ ...km)

### Fluid saturation



fully saturated

patchy saturated  
(mm...km)



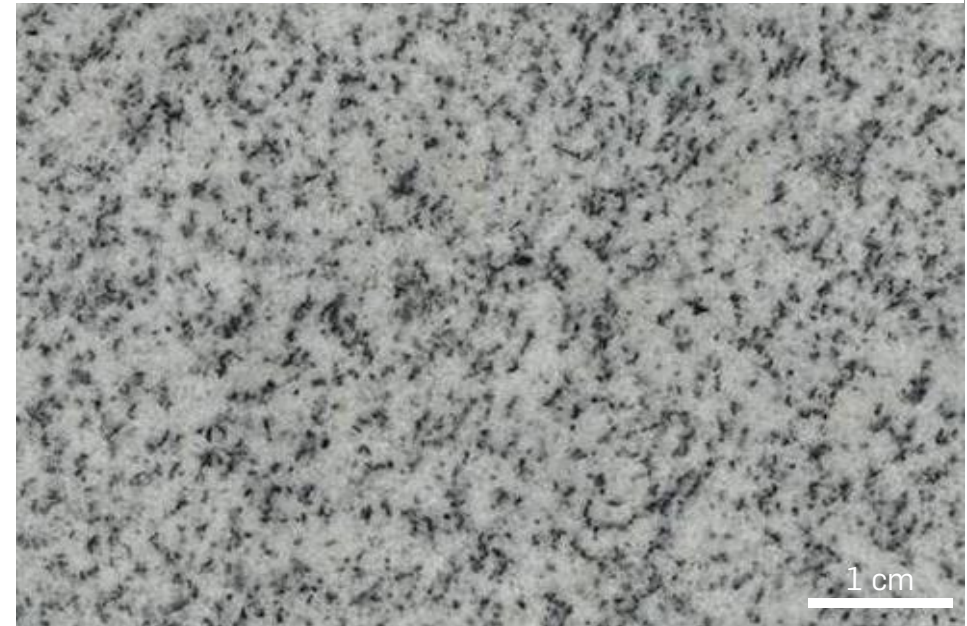
## Solnhofen limestone



<http://geo.hlipp.de/photo/142>

- Low attenuation
- Easy preparation of sample material
- Natural isotropic fracture roughness

## Padang granodiorite



[http://eurasian.com/china/granite/images/g633\\_500.jpg](http://eurasian.com/china/granite/images/g633_500.jpg)

- Rather free of cracks/fractures
- Geothermal relevance („hot rocks“)
- Represents crystal basement



## Cyclic axial loading

Samples contain an idealized fault, created by stacking two sample discs on top of each other.



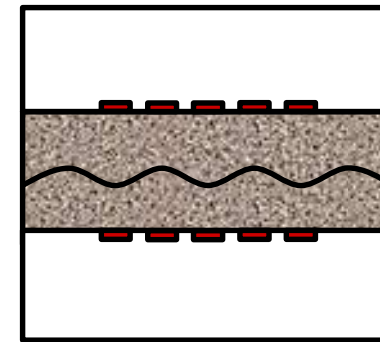
Transmission properties of fractured rocks in dependence of:

- normal stress
- frequency
- reflection and transmission angle



axial dynamic load

$f < 10$  Hz



P- and S-wave transducers

$f > 100$  kHz



axial static load

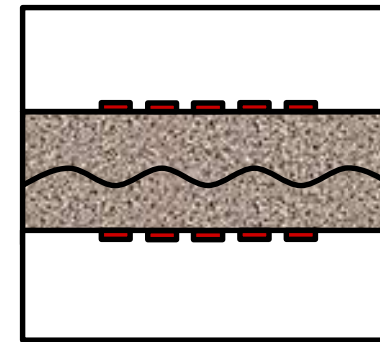


## Experimental settings

- Characterization of single intact and stacked fractured rock
- Various frequencies and axial stresses
- Defined fracture roughness
  - creation of isotropic roughness
  - 3D image analysis
- Fracture-filling fluids with different viscosities
  - water:  $\eta_{\text{water}} \sim 10^{-3} \text{ Pa}\cdot\text{s}$
  - silicone oil:  $\eta_{\text{silicone}} \sim 10^2 \dots 10^6 \cdot \eta_{\text{water}}$

axial dynamic load

$f < 10 \text{ Hz}$



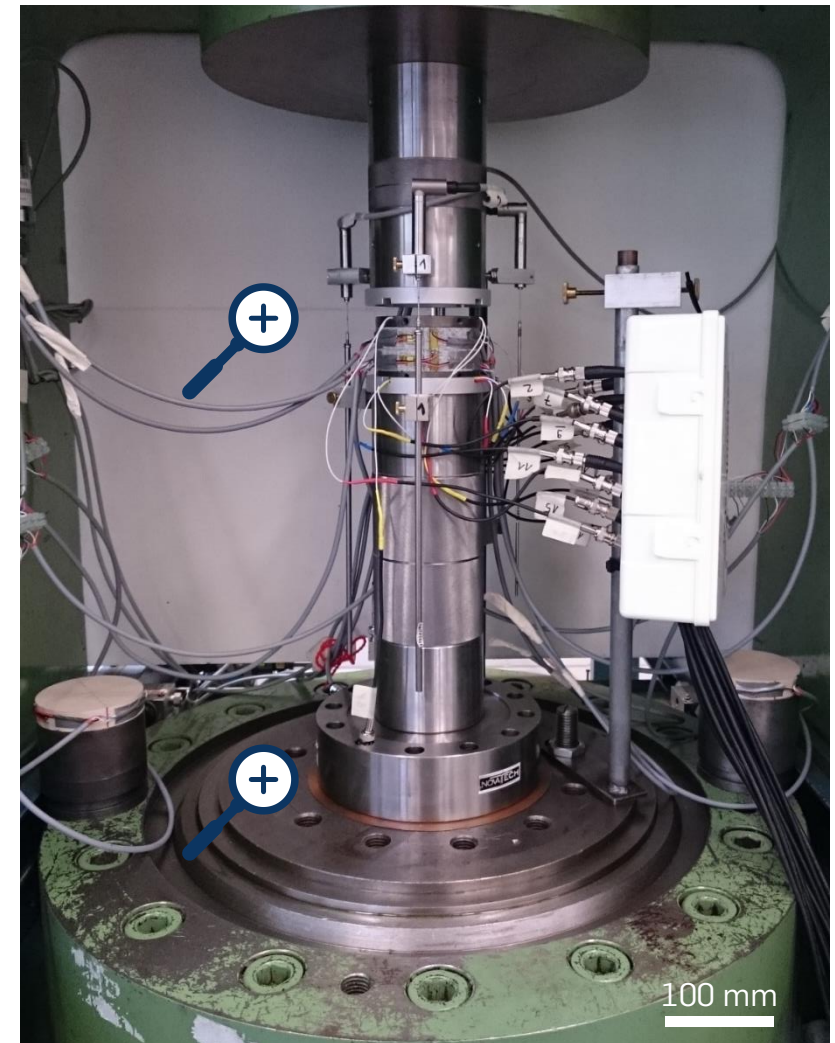
P- and S-wave transducers

$f > 100 \text{ kHz}$



## Mechanical characterization

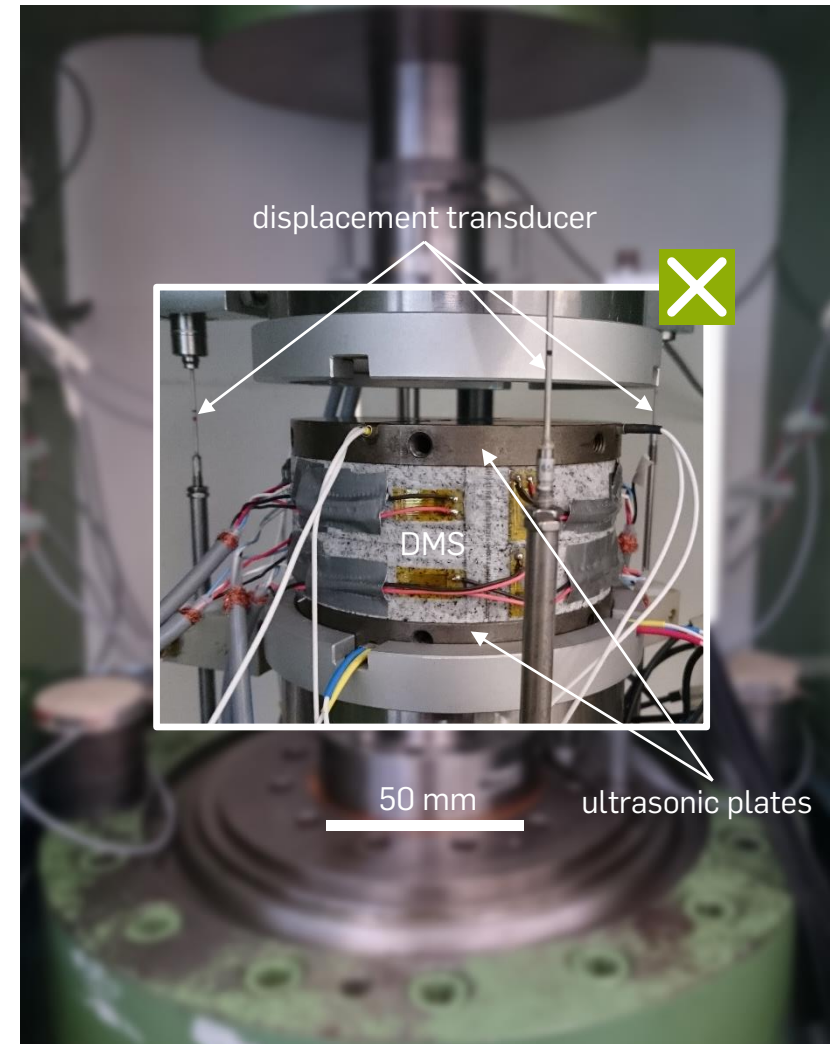
- Two stacked sample discs
  - diameter: 100 mm
  - height: 20 mm
- Axial loading piston and load cell
- Three displacement transducers (LVDT)
  - arranged at an angle of  $120^\circ$
- Four strain gauges (DMS) on each sample
  - measure longitudinal and lateral strain
  - temperature compensation





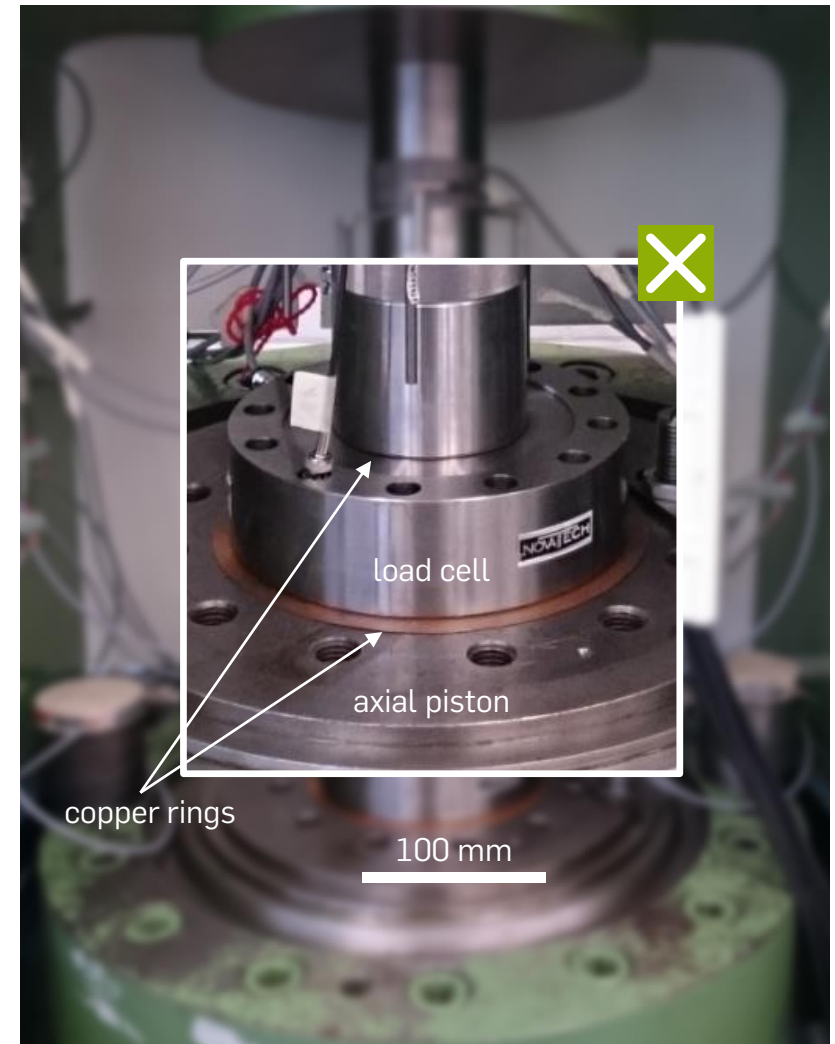
## Mechanical characterization

- Two stacked sample discs
  - diameter: 100 mm
  - height: 20 mm
- Axial loading piston and load cell
- Three displacement transducers (LVDT)
  - arranged at an angle of  $120^\circ$
- Four strain gauges (DMS) on each sample
  - measure longitudinal and lateral strain
  - temperature compensation

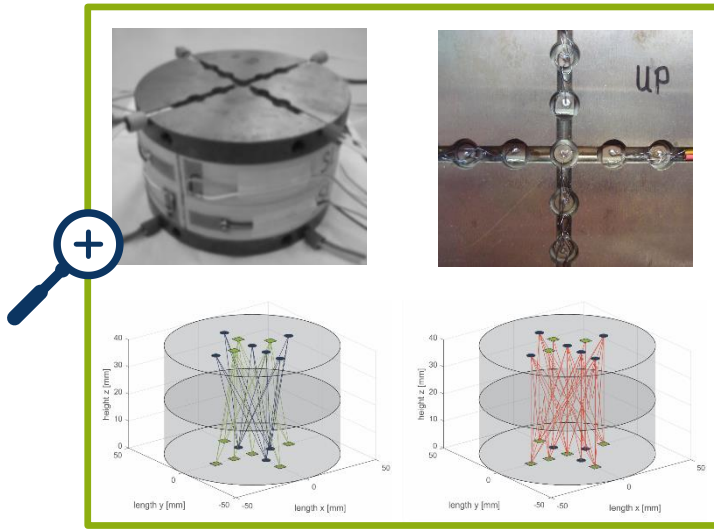


## Mechanical characterization

- Two stacked sample discs
  - diameter: 100 mm
  - height: 20 mm
- Axial loading piston and load cell
- Three displacement transducers (LVDT)
  - arranged at an angle of  $120^\circ$
- Four strain gauges (DMS) on each sample
  - measure longitudinal and lateral strain
  - temperature compensation



## Acoustical characterization

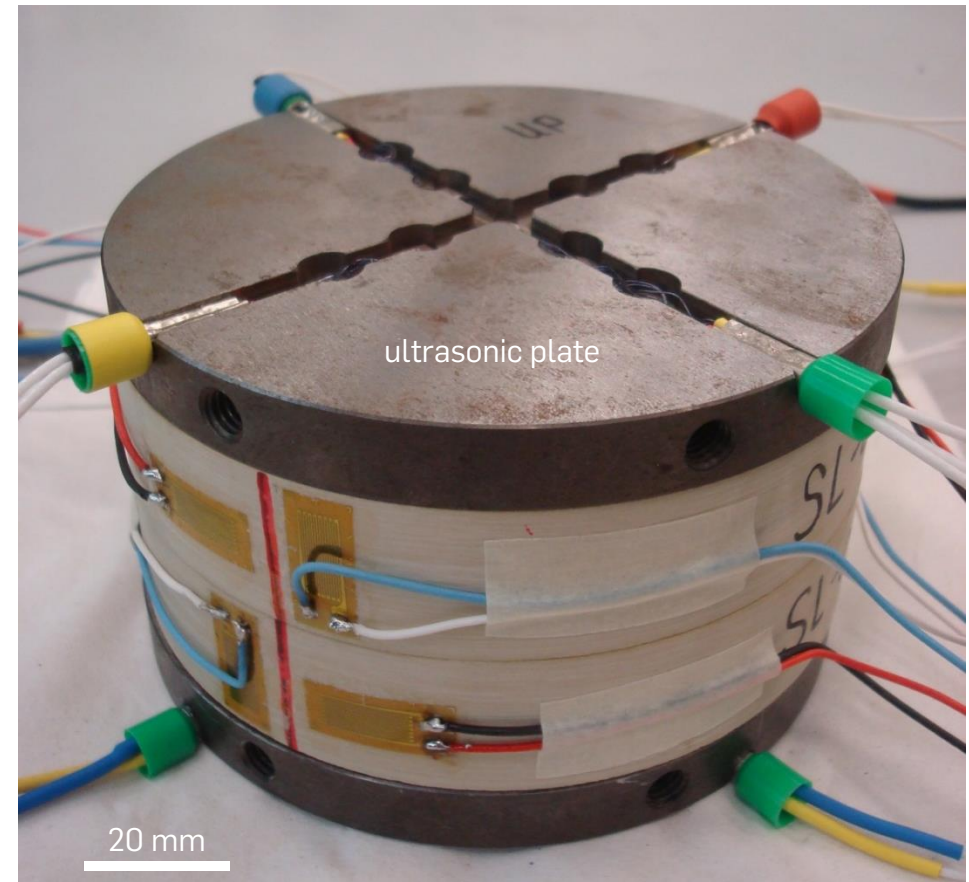


Upper ultrasonic plate:

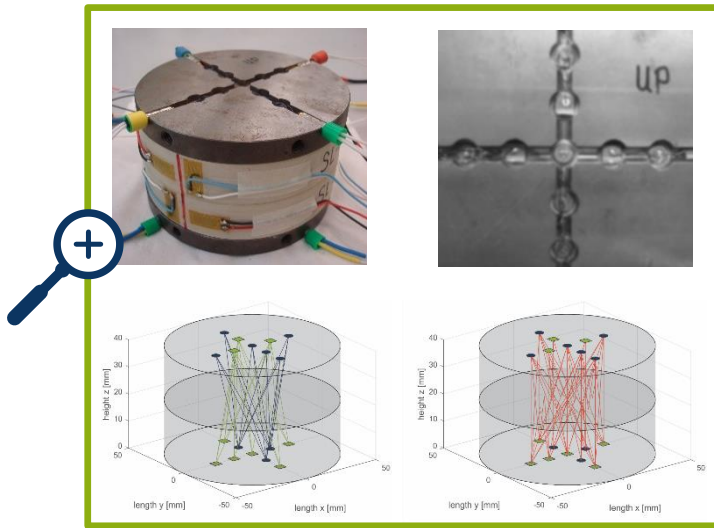
- 6 **P**-wave & 3 **S**-wave sensors

Lower ultrasonic plate:

- 3 **P**-wave & 6 **S**-wave sensors



## Acoustical characterization

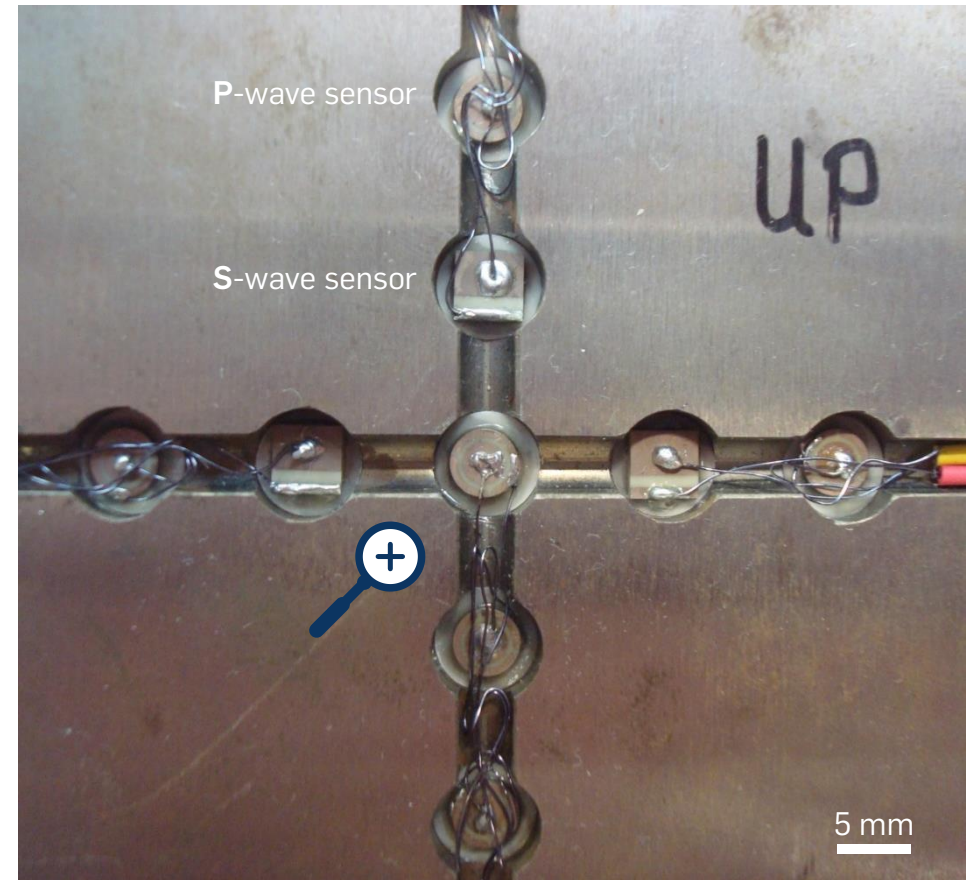


Upper ultrasonic plate:

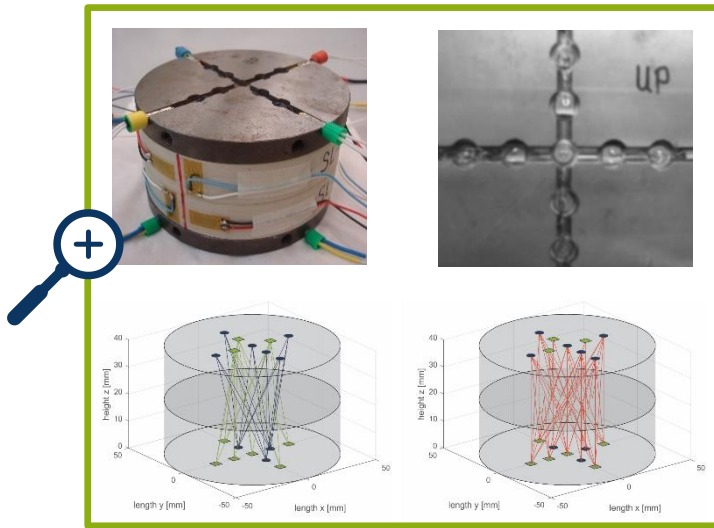
- 6 **P**-wave & 3 **S**-wave sensors

Lower ultrasonic plate:

- 3 **P**-wave & 6 **S**-wave sensors



## Acoustical characterization

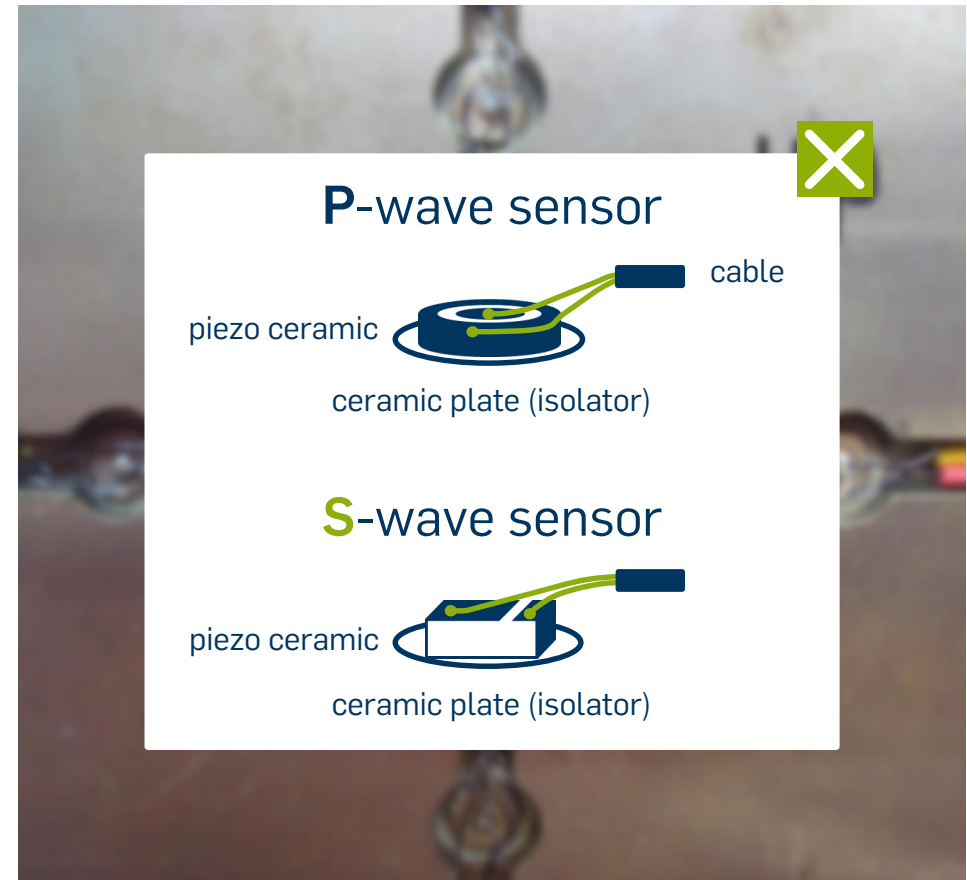


Upper ultrasonic plate:

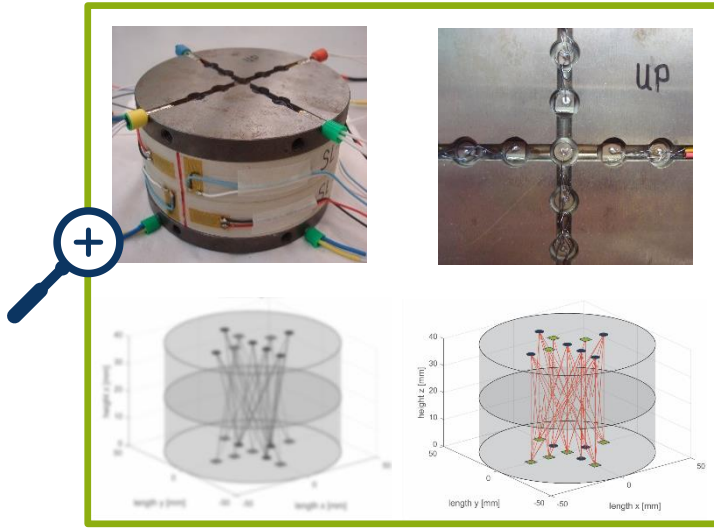
- 6 **P**-wave & 3 **S**-wave sensors

Lower ultrasonic plate:

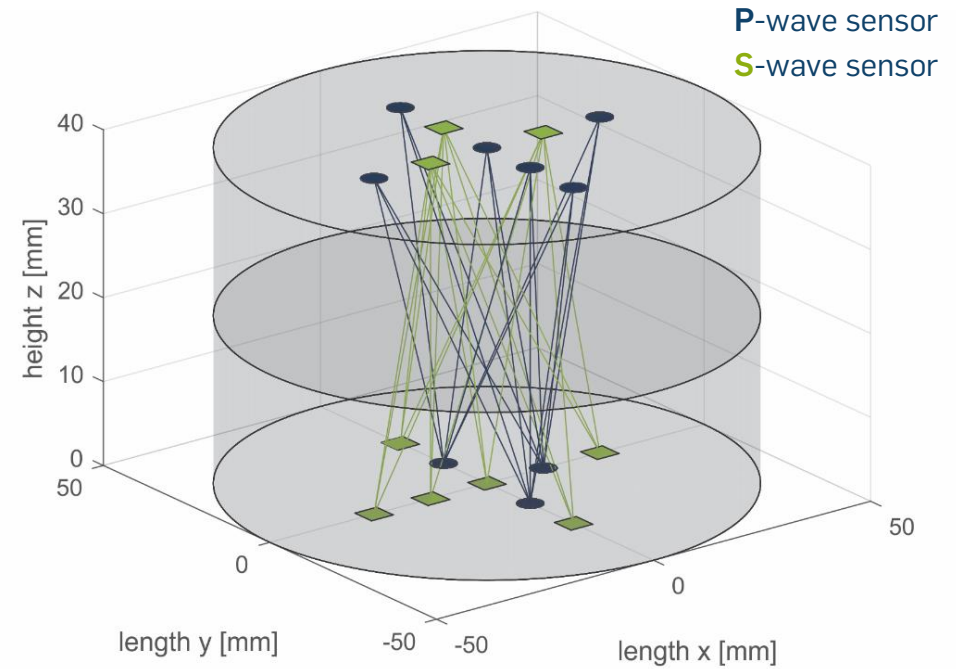
- 3 **P**-wave & 6 **S**-wave sensors



## Acoustical characterization



### Transmission ray paths



### Transmission angles:

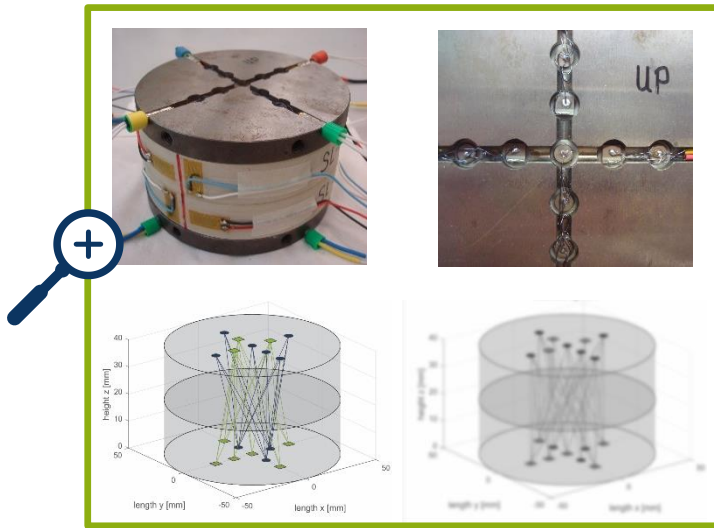
- 0, 17.6, 24.2, 32.4, 35.3 & 43.6°

### Reflection angles:

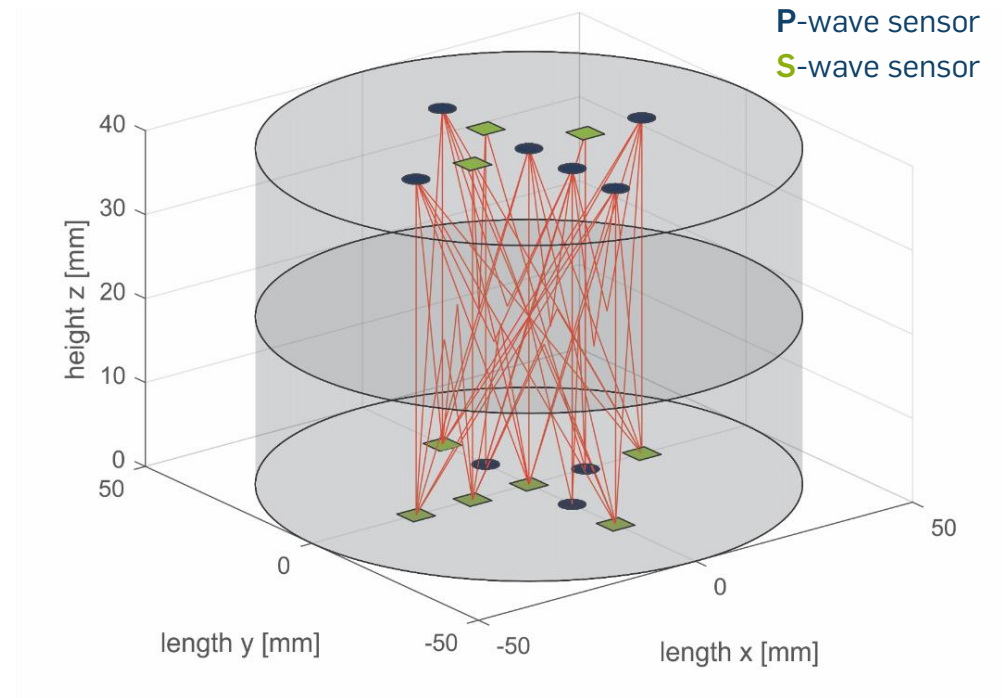
- 0, 17.6, 24.2, 32.4, 35.3, 41.9, 43.6 & 51.7°



## Acoustical characterization



### Reflection ray paths



Transmission angles:

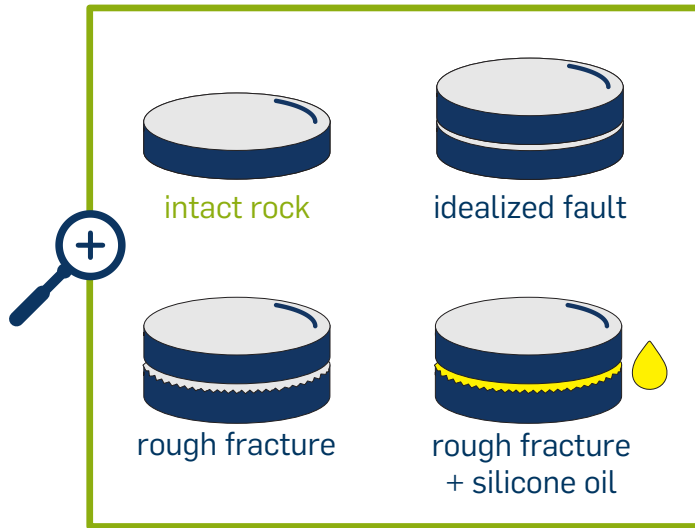
- 0, 17.6, 24.2, 32.4, 35.3 & 43.6°

Reflection angles:

- 0, 17.6, 24.2, 32.4, 35.3, 41.9, 43.6 & 51.7°

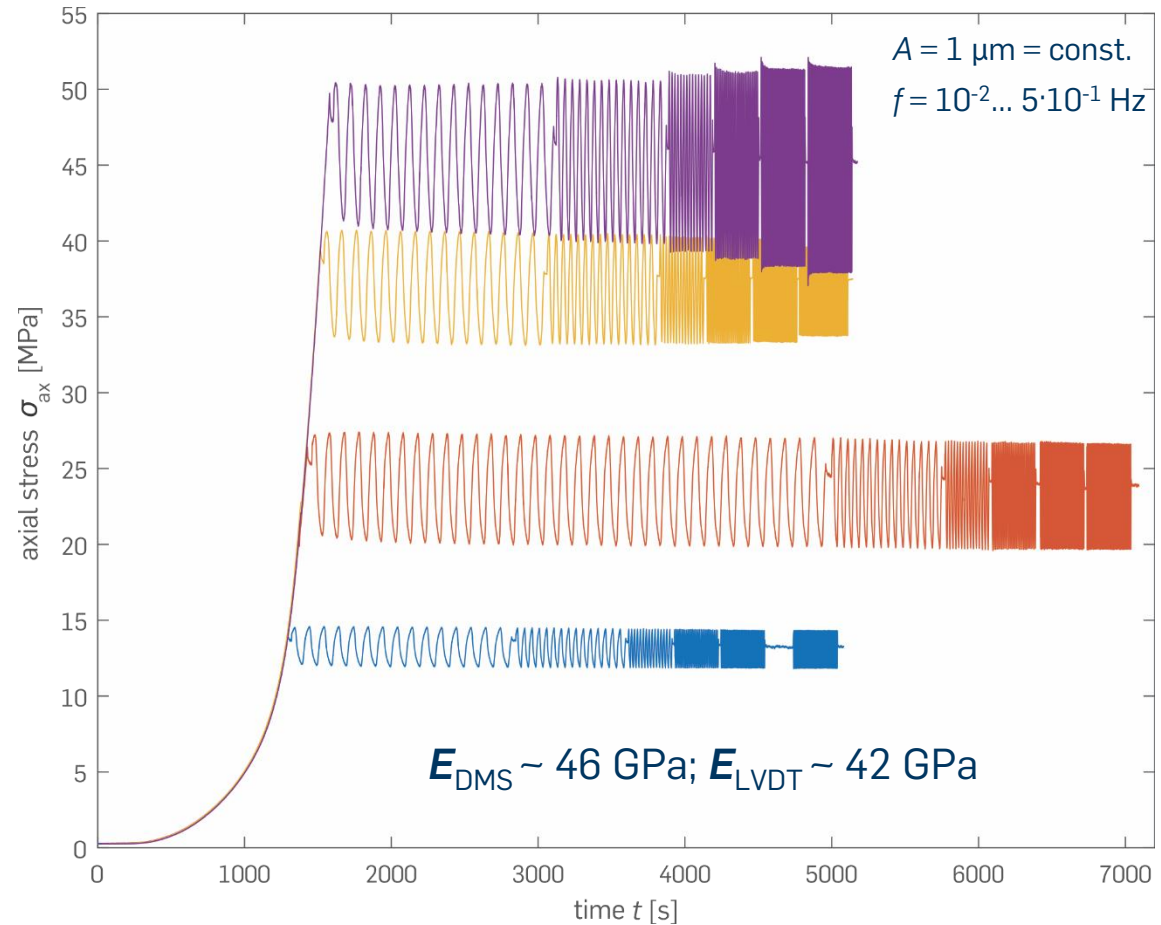


## Padang granodiorite



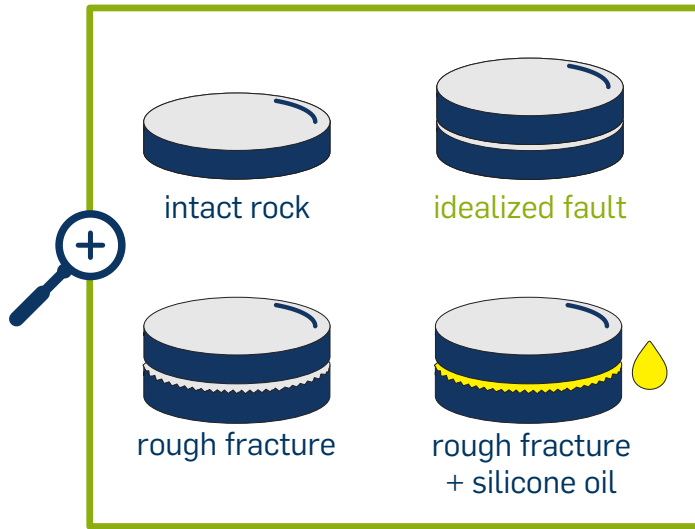
- Axial stiffness increases with increasing load
- Stress relaxation is slightly affected by stress state

### Intact rock



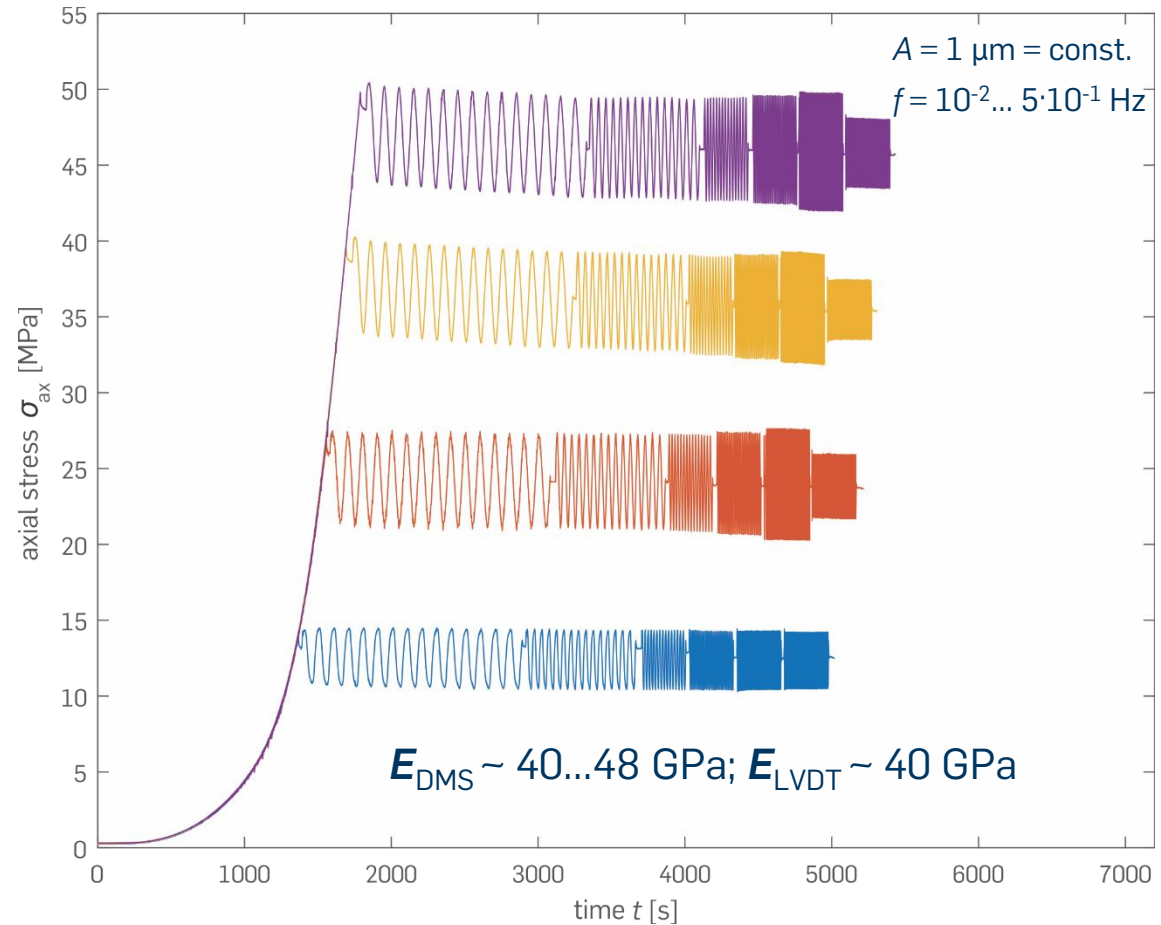


## Padang granodiorite

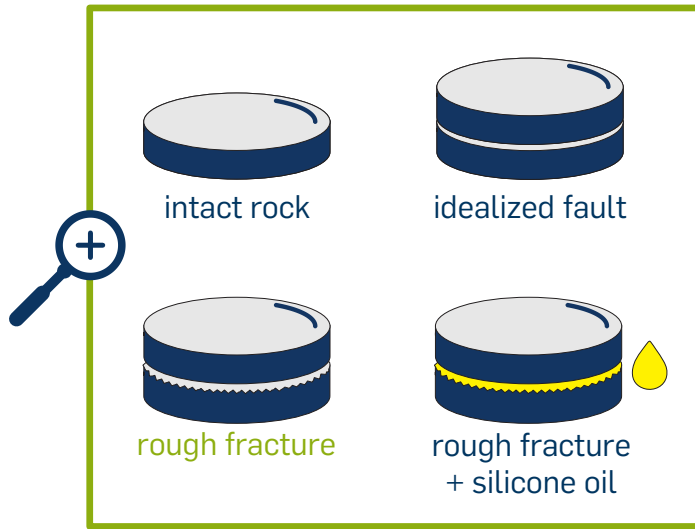


- Total stiffness decreases due to idealized fault
- Idealized fault has a minor effect on Young's modulus

## Idealized fault

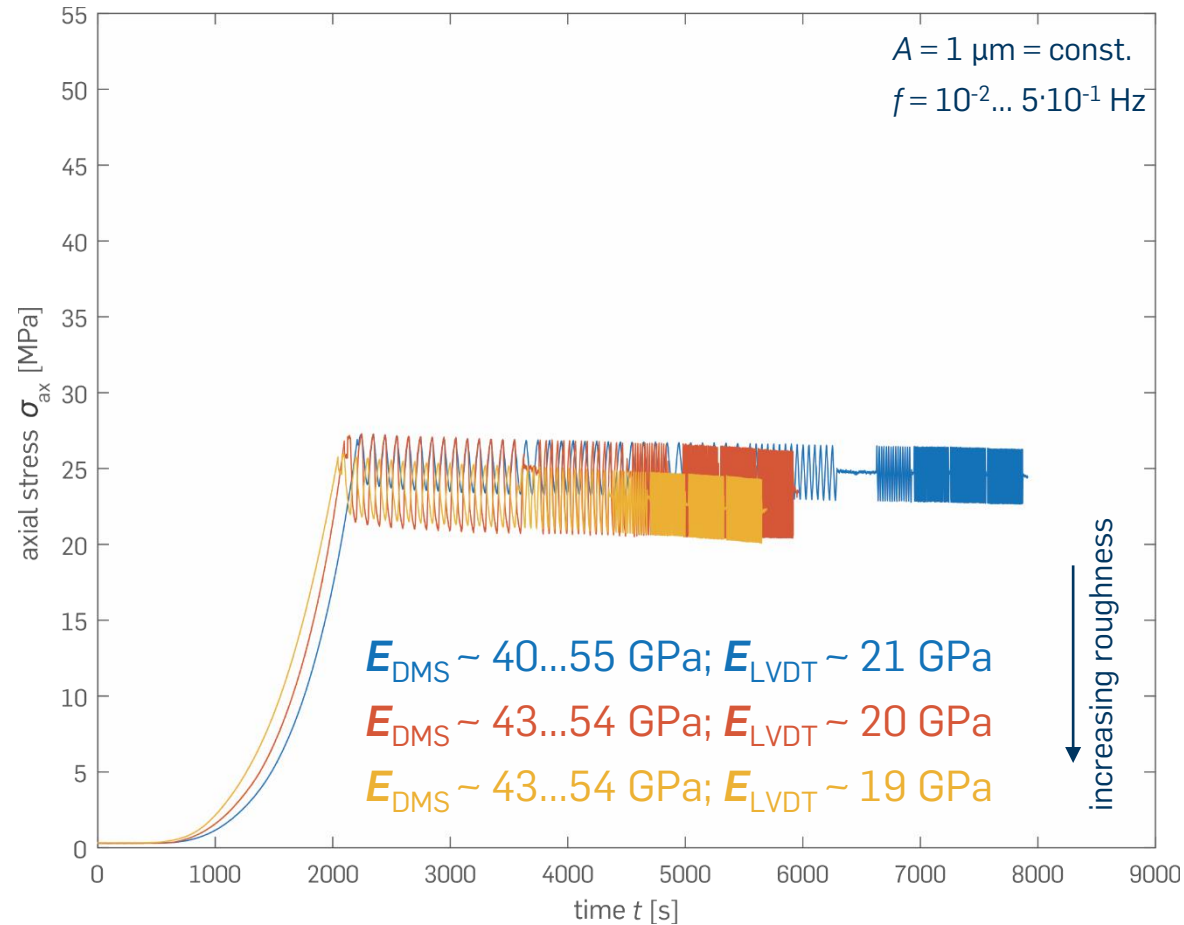


## Padang granodiorite

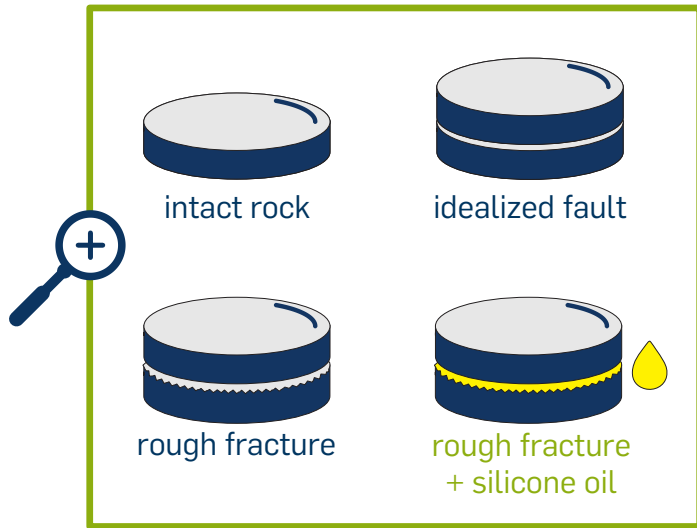


- At the same axial stress, roughness variation has a minor influence on the stiffness

## Idealized fault with rough fracture

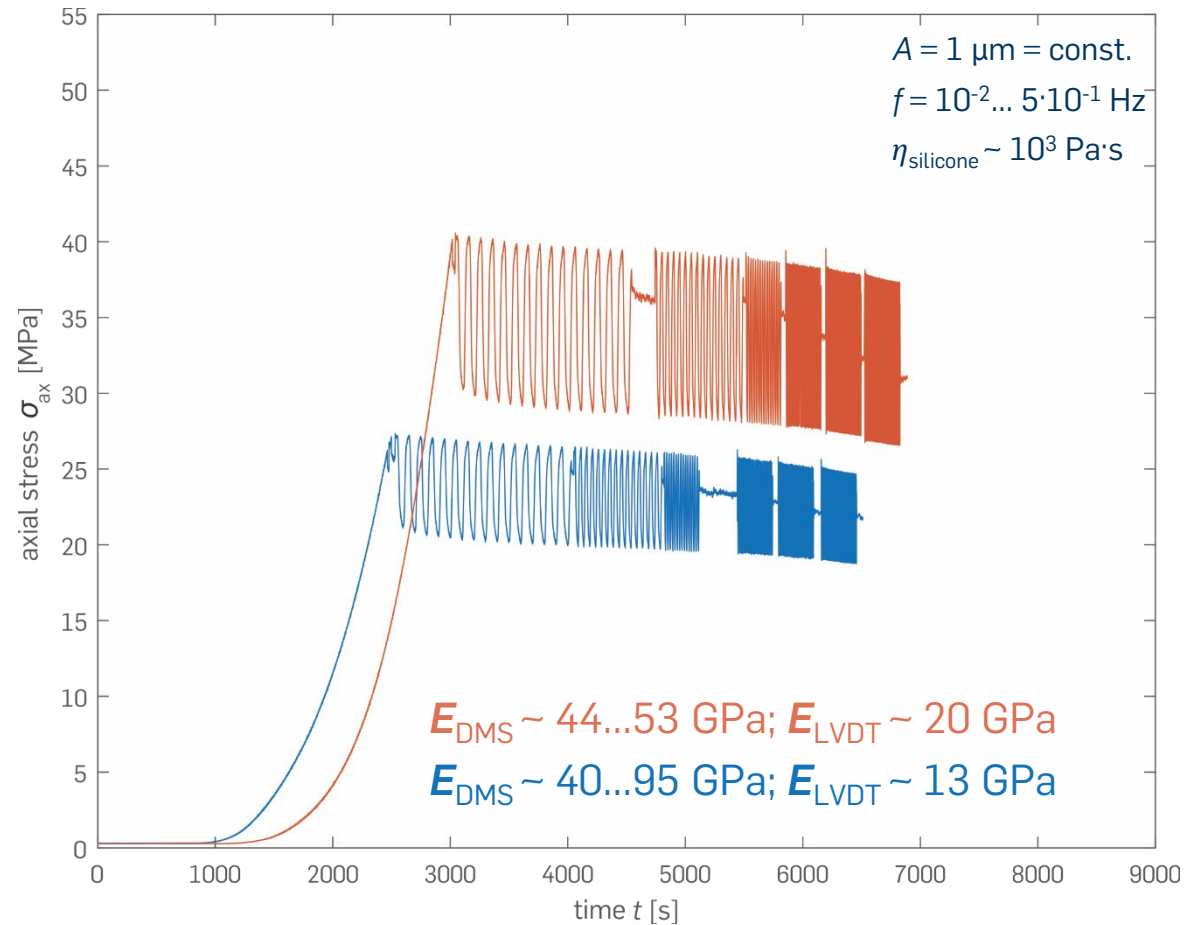


## Padang granodiorite



- Viscous fluid delays loading, decreases total stiffness and enlarges relaxation
- Strain gauges yield increased apparent stiffnesses

## Idealized fault with rough fracture and viscous oil

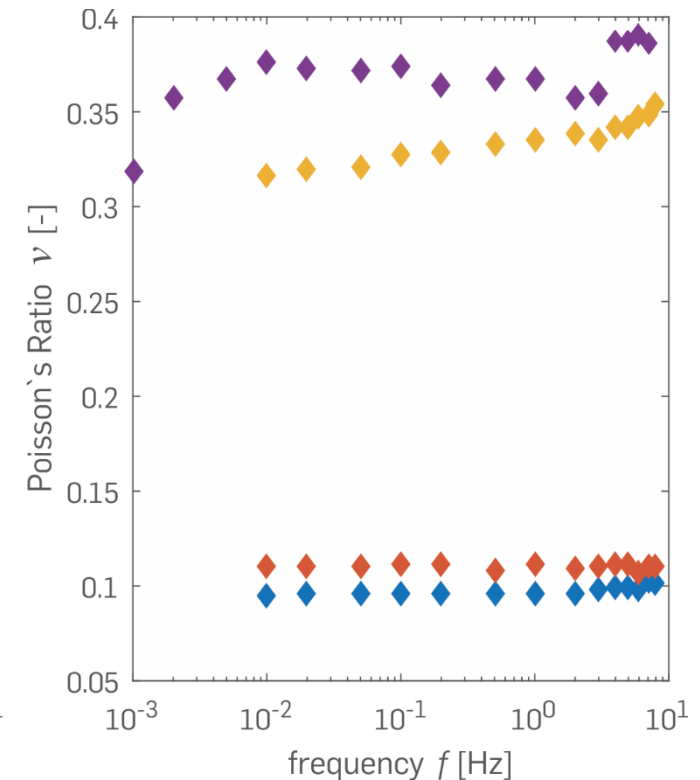
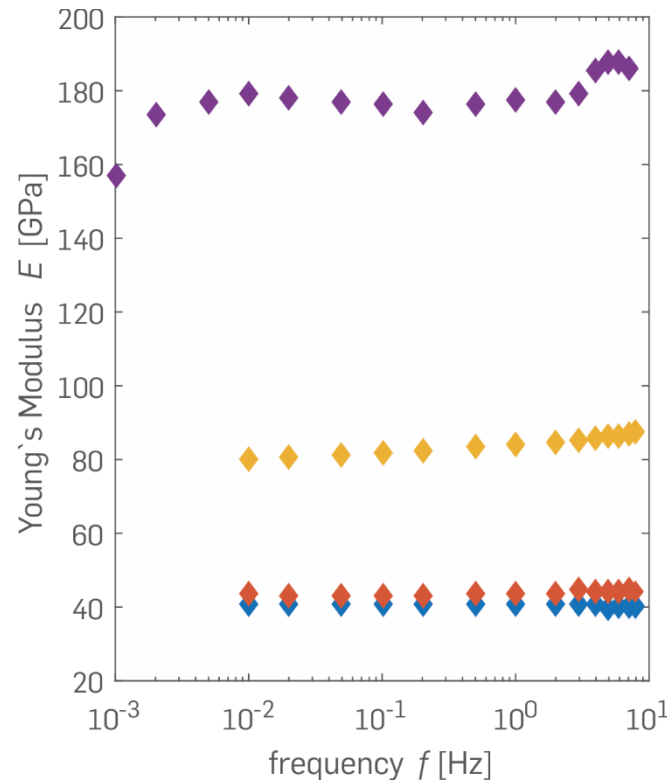


## Padang granodiorite

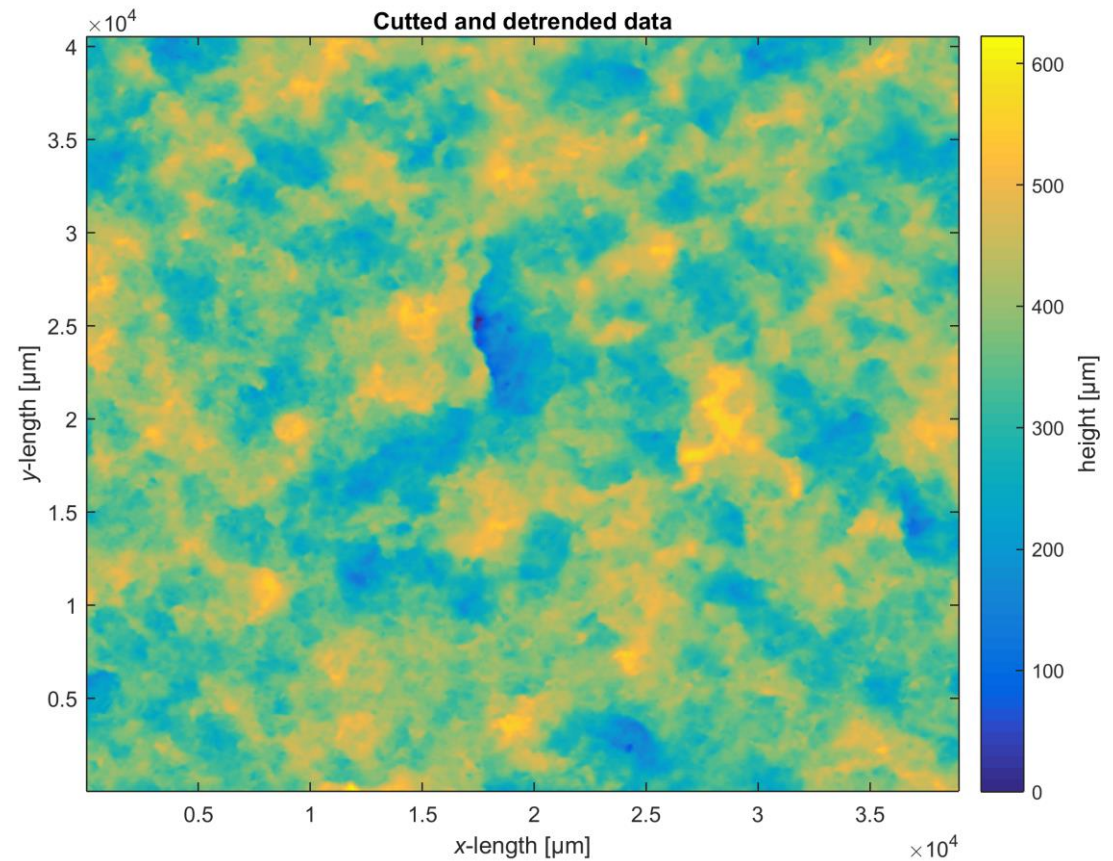
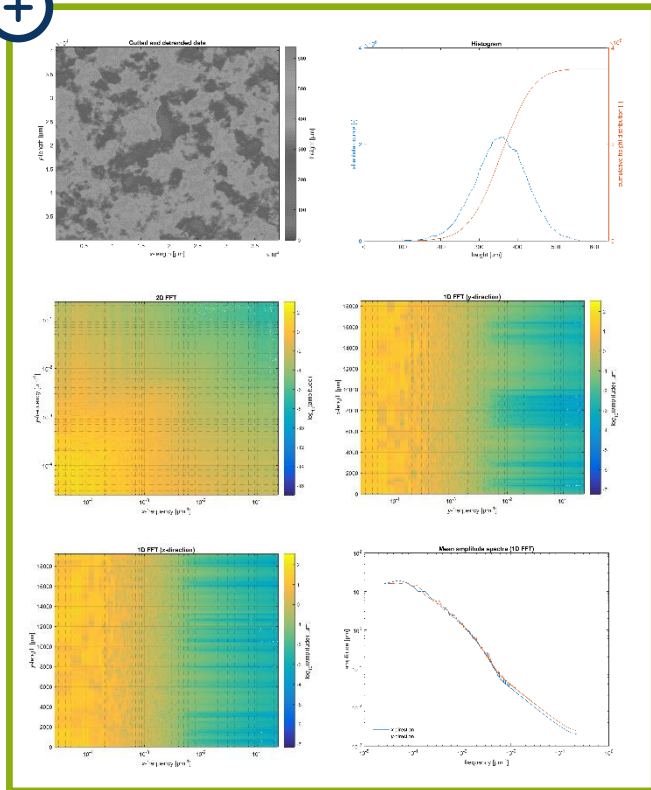
### Elastic properties of sample discs ( $\sigma_{ax} = 25$ MPa)

intact rock | idealized fault | rough fracture | rough fracture + silicone oil

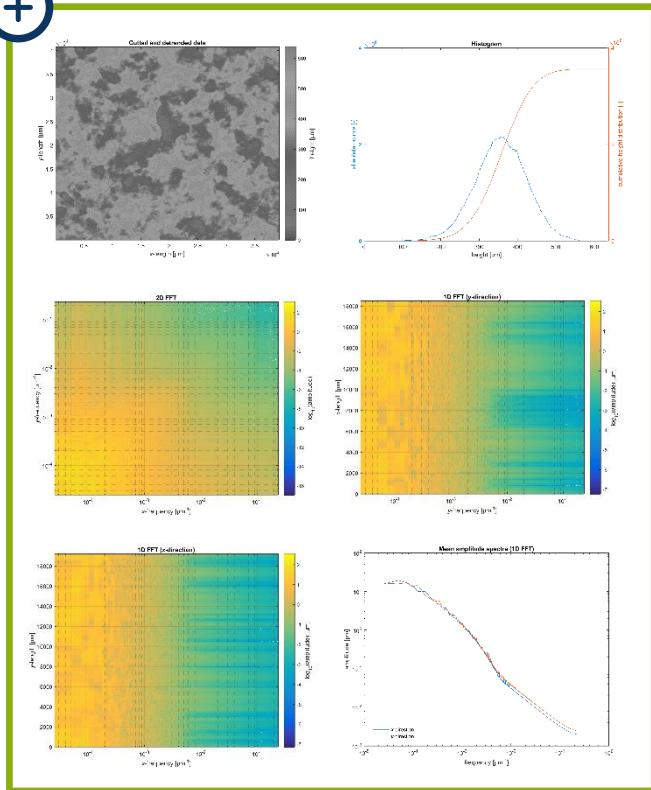
- Small dispersion of Young's modulus and Poisson's ratio
- Rough fractures and the effect of viscous fluids yield increased apparent elastic properties



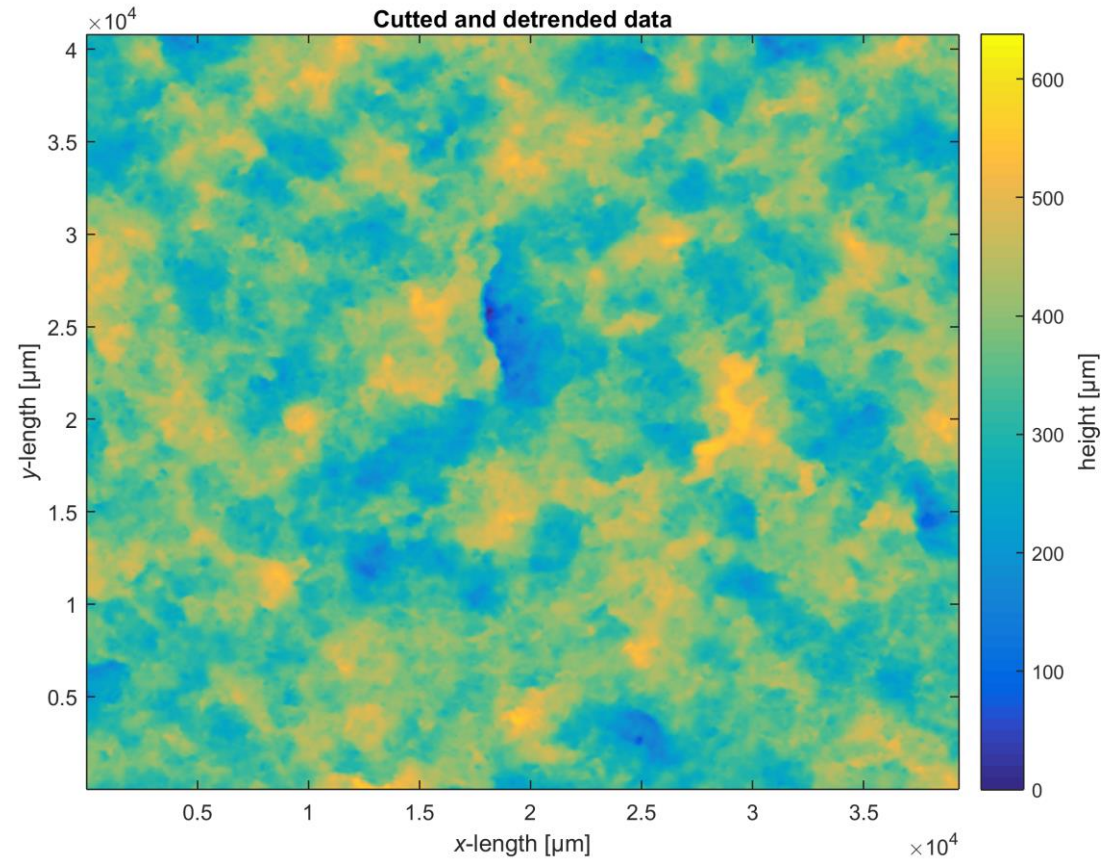
## Padang granodiorite



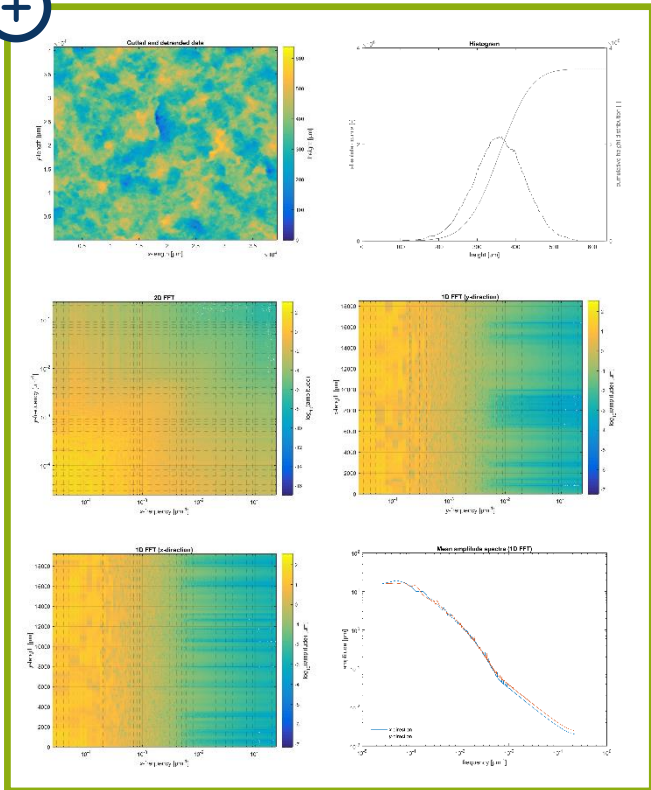
## Padang granodiorite



before ← after



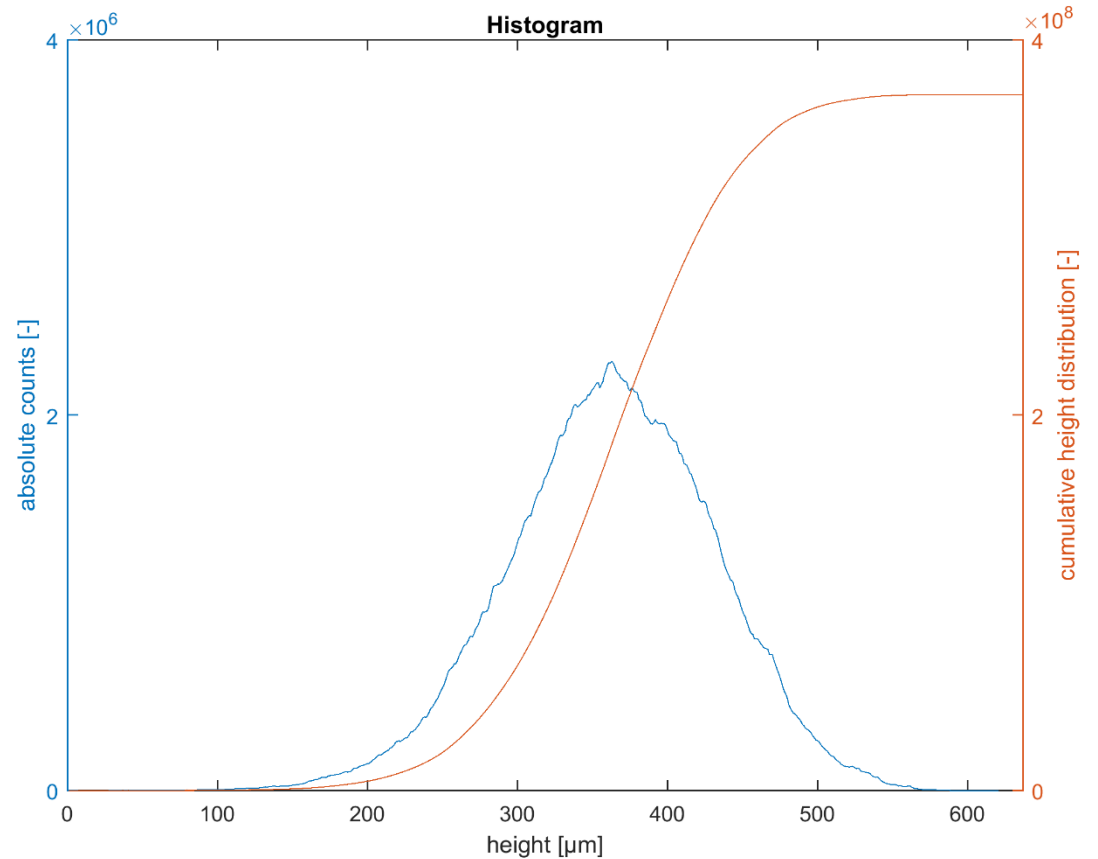
## Padang granodiorite



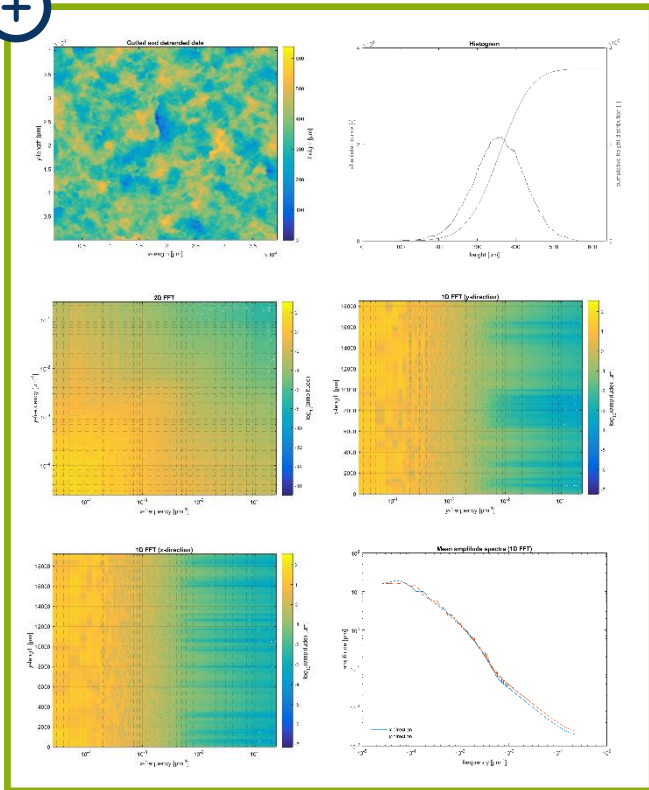
before



after



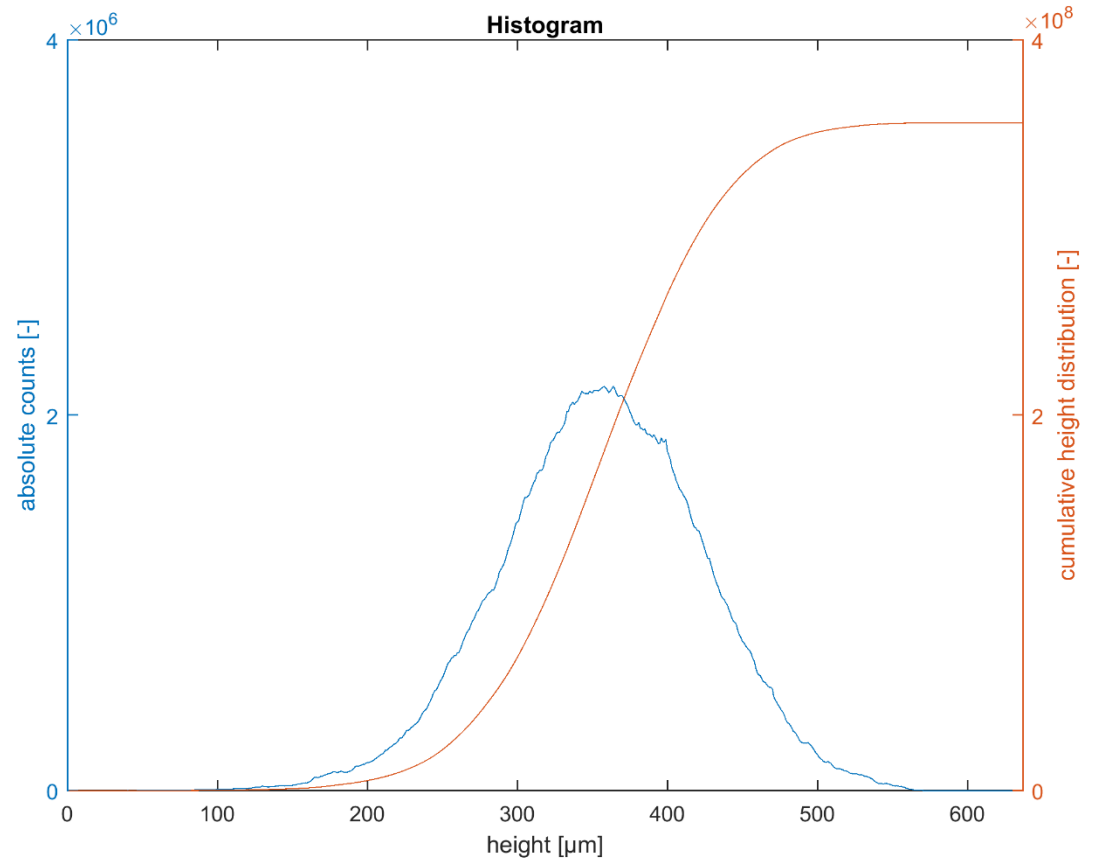
## Padang granodiorite



before

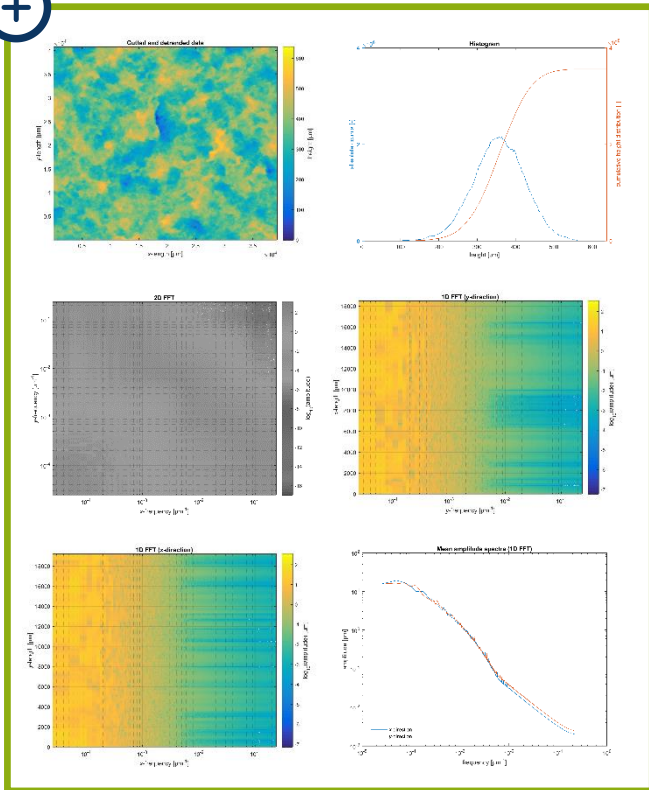


after





## Padang granodiorite

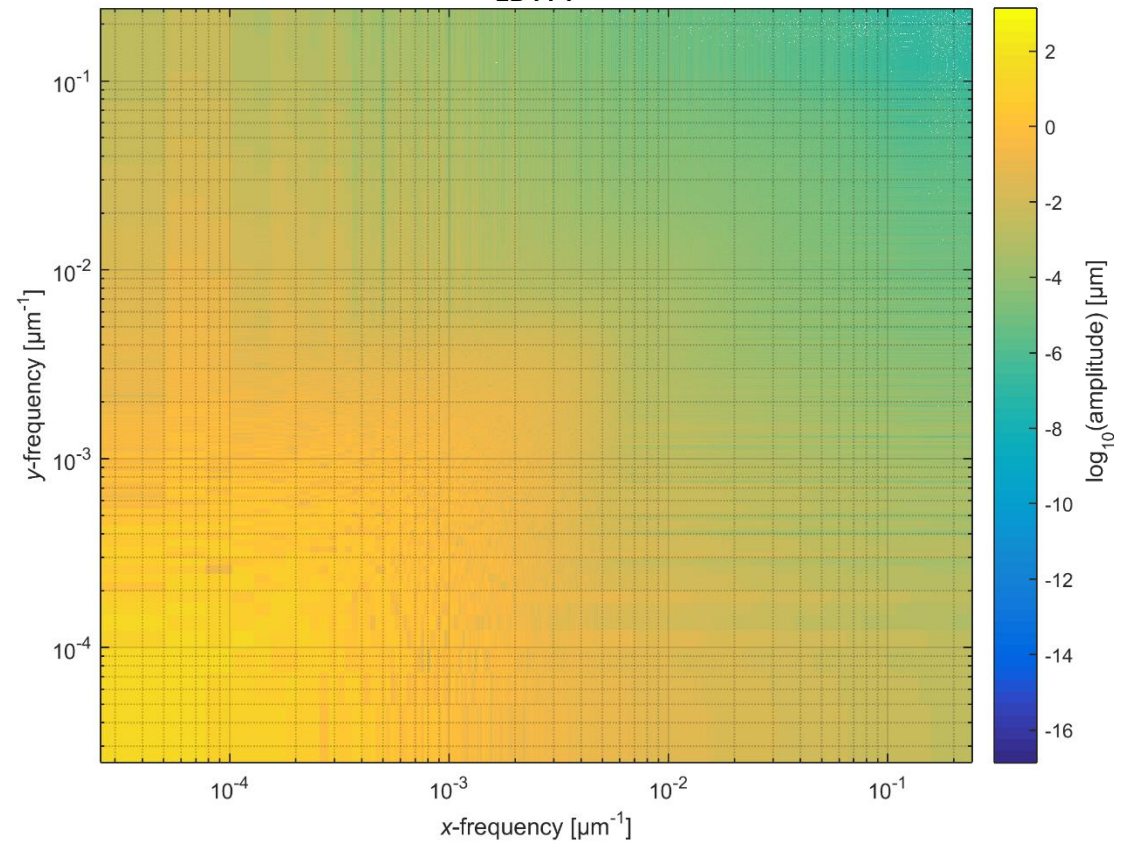


before

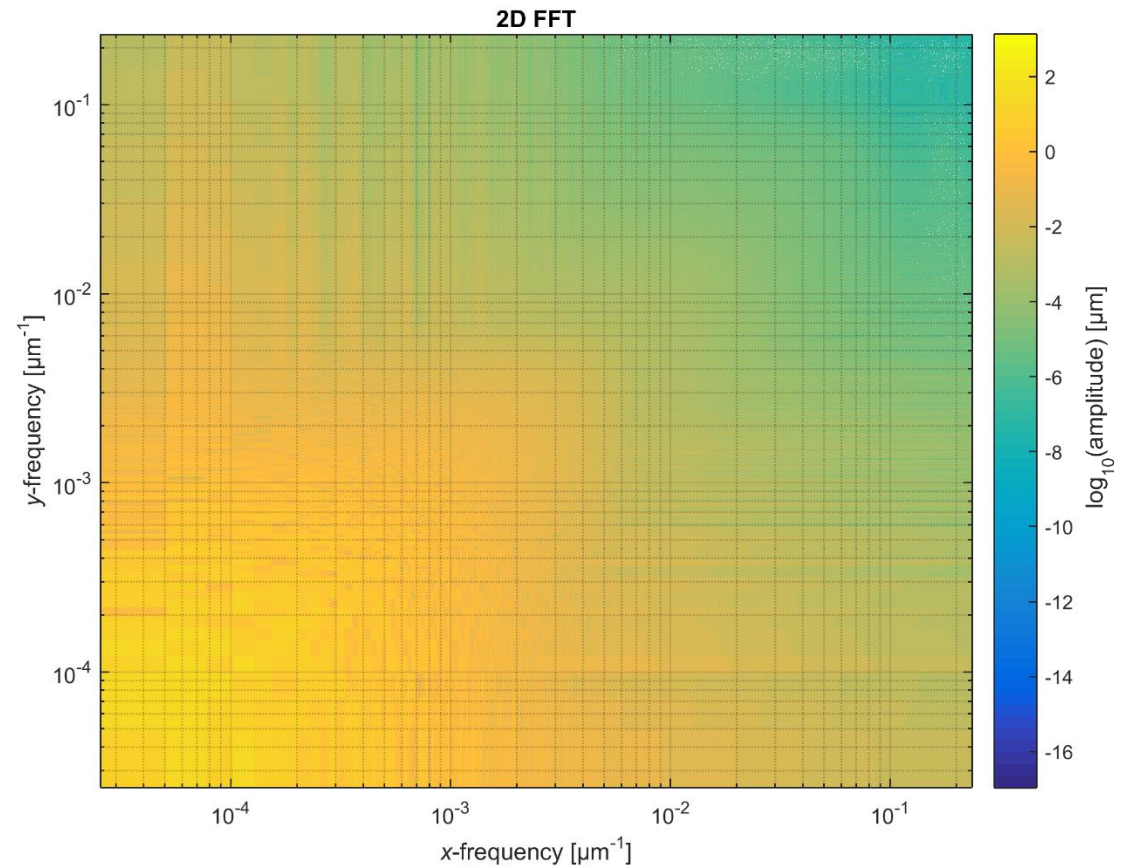
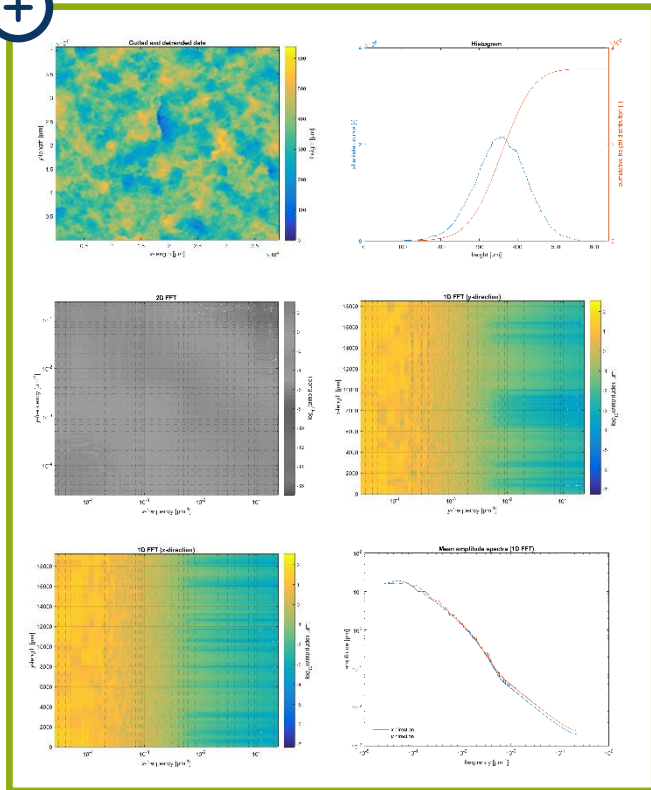


after

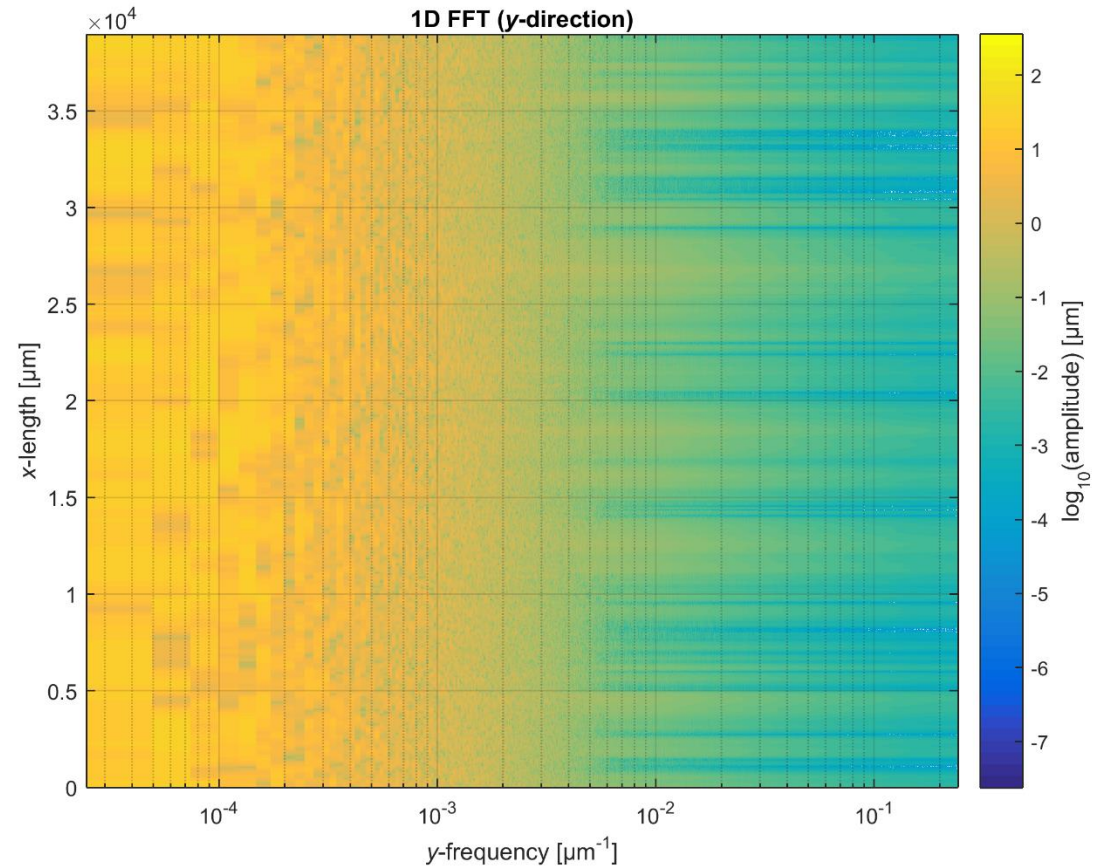
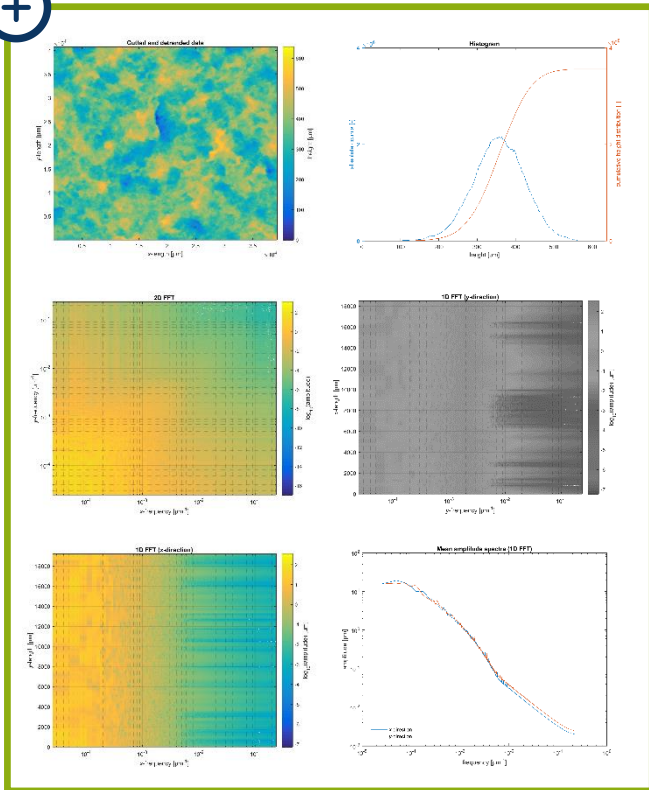
2D FFT



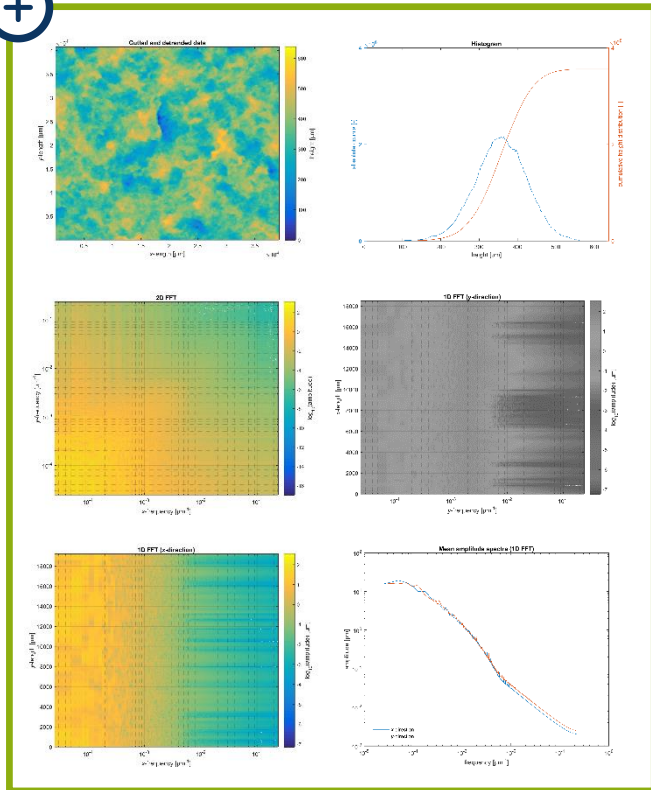
## Padang granodiorite



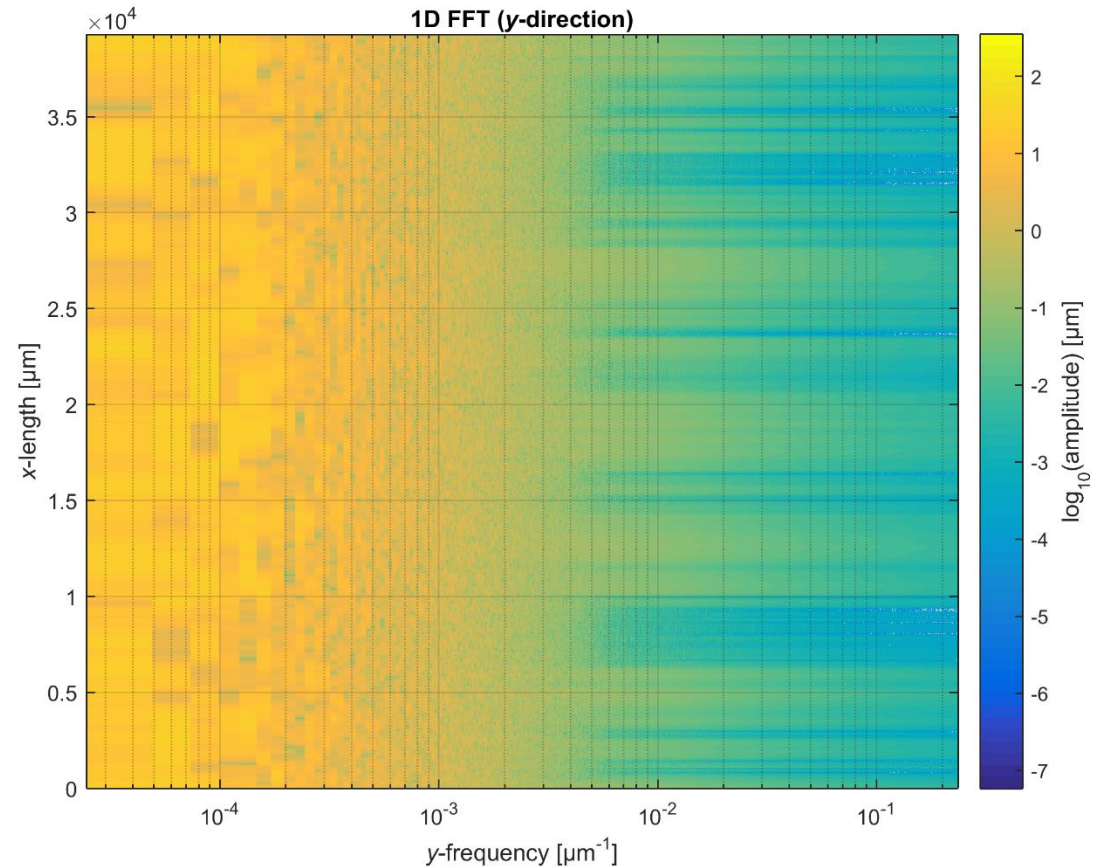
## Padang granodiorite



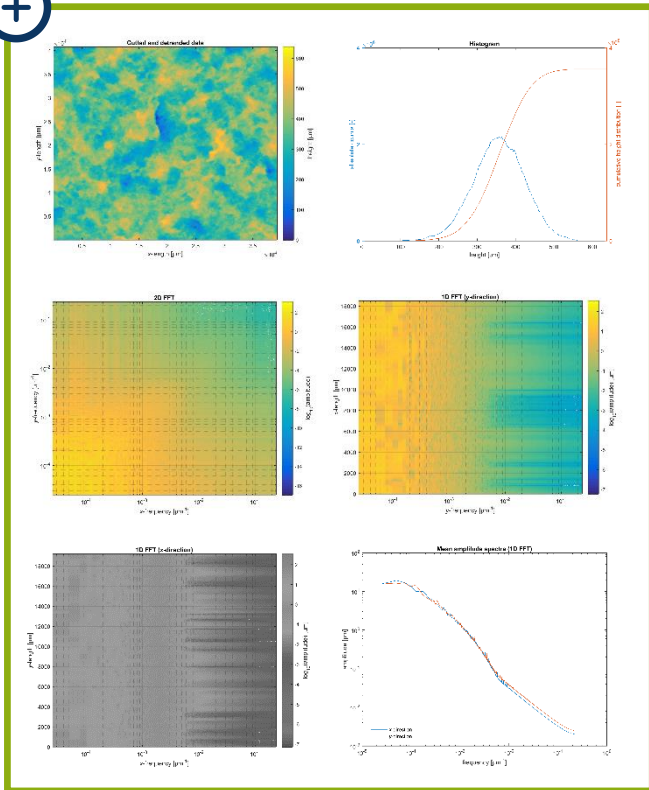
## Padang granodiorite



before ← after



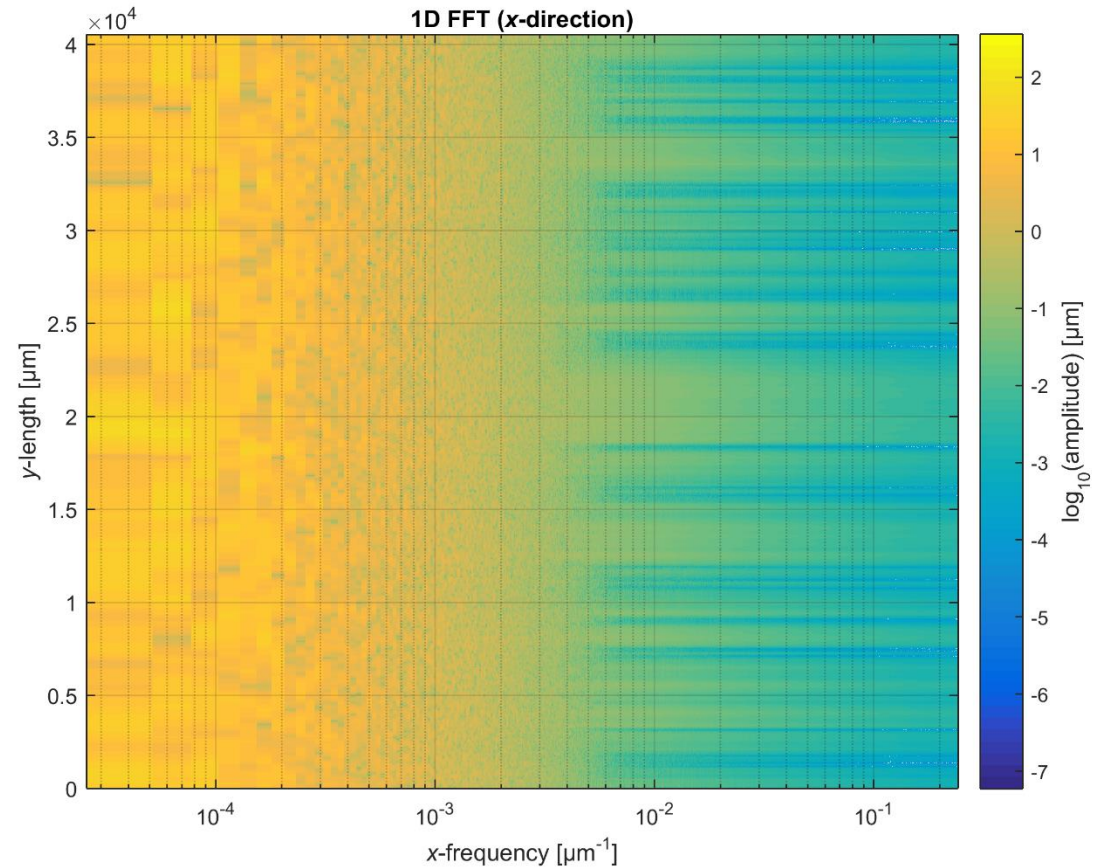
## Padang granodiorite



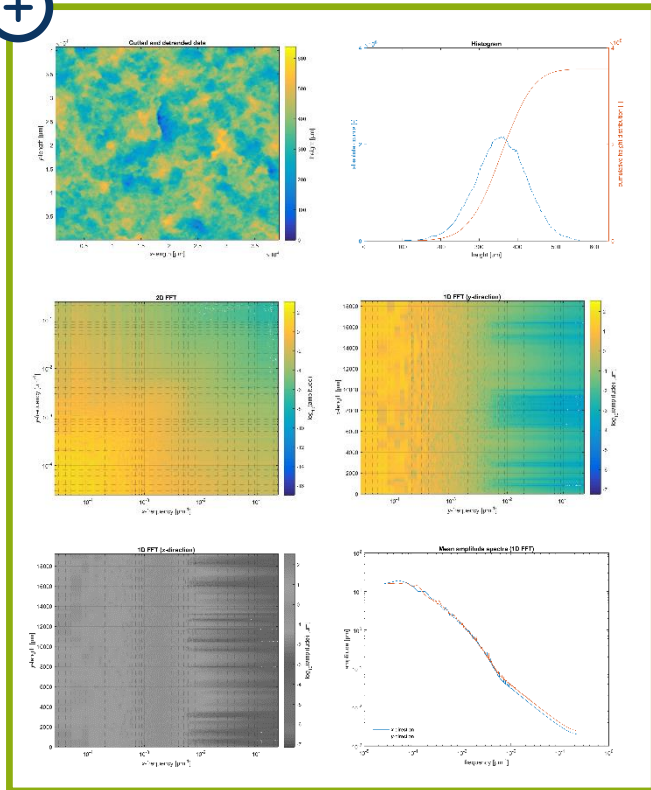
before



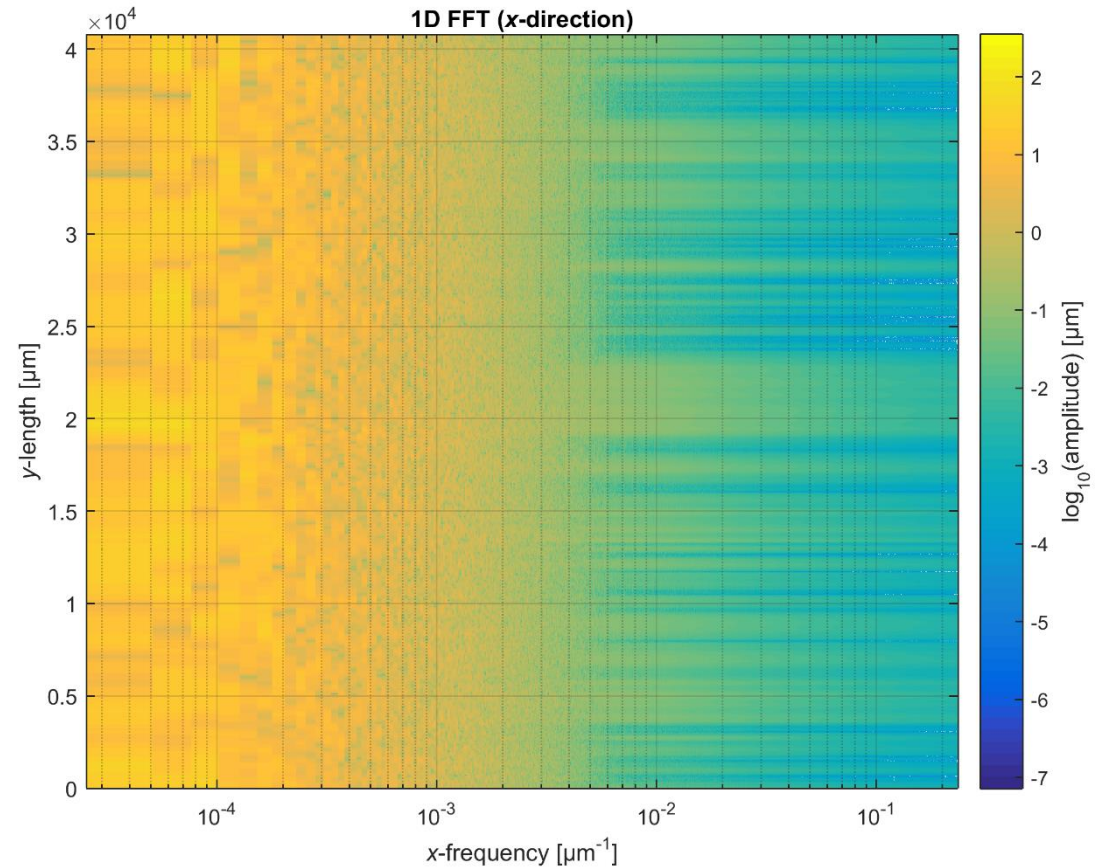
after



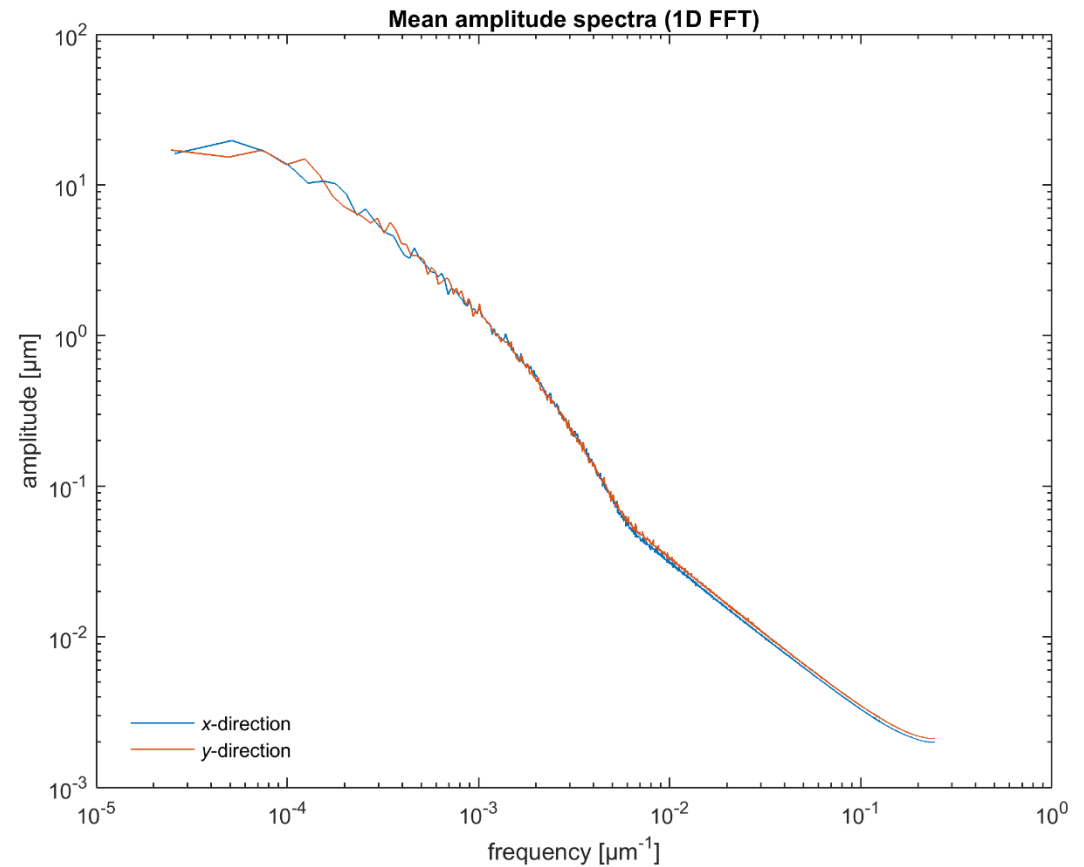
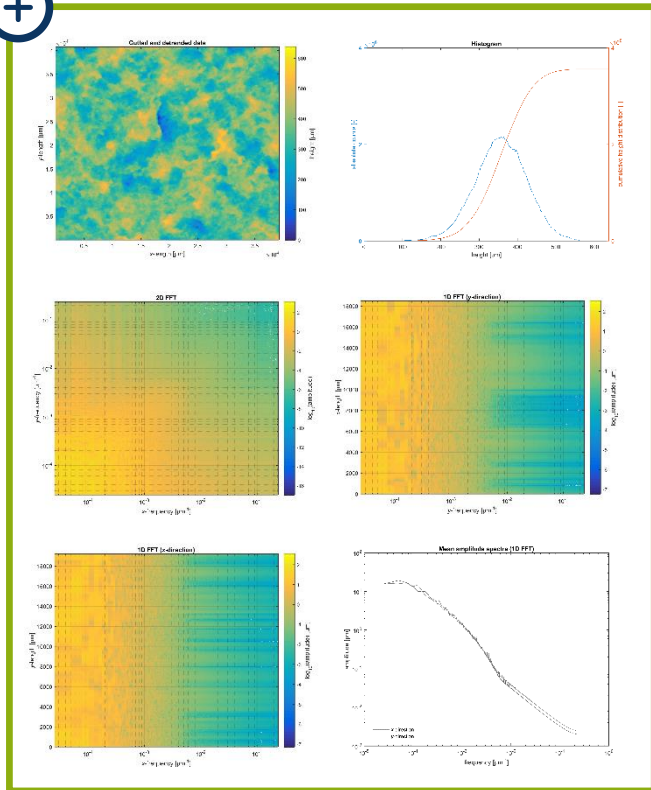
## Padang granodiorite



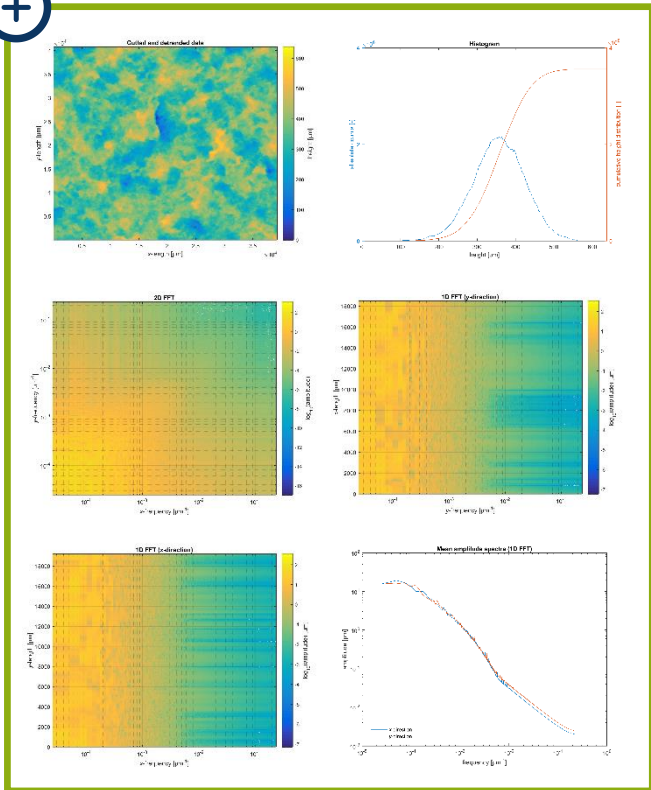
before ← after



## Padang granodiorite



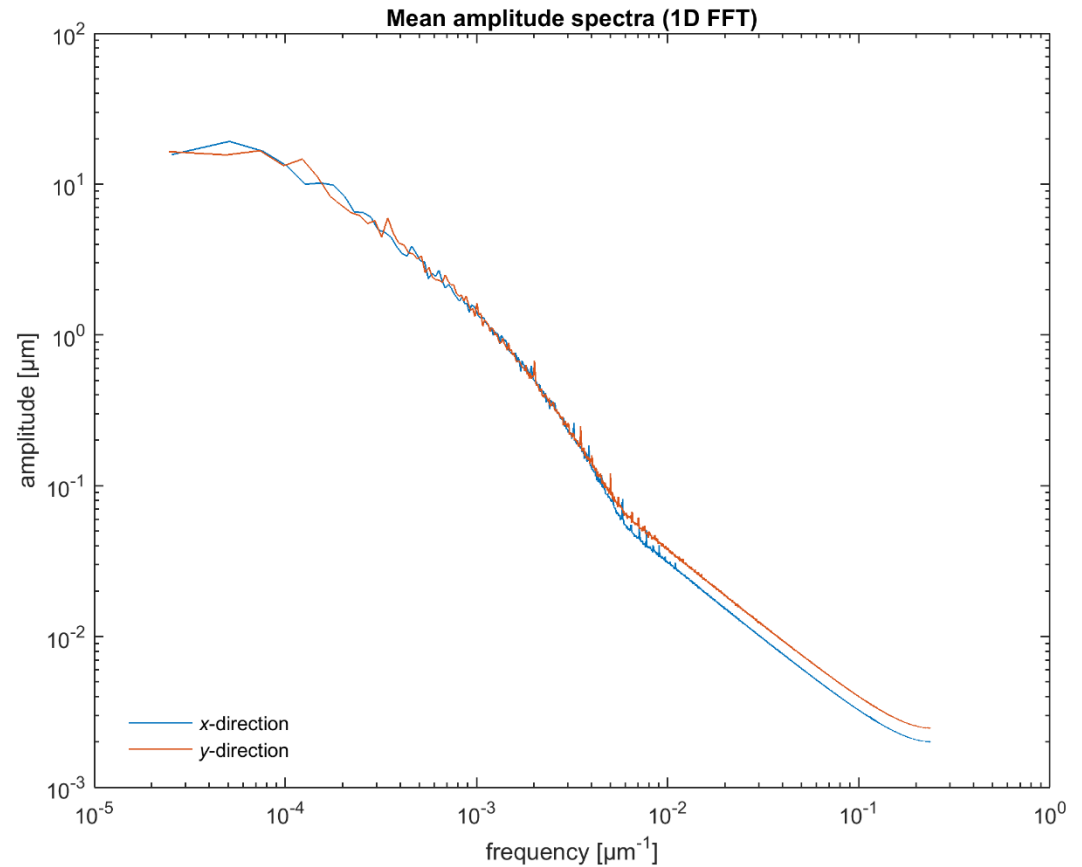
## Padang granodiorite



before



after



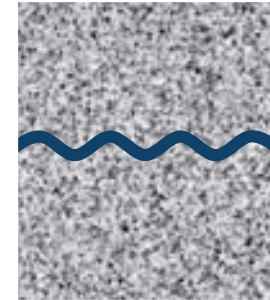


- Stress **relaxation**:
  - elastic properties depend on stress state and degree of relaxation
- Frequency **dispersion** in elastic properties:
  - small dispersion in the frequency range between  $10^{-3}$  and  $10^1$  Hz
- Effect of **idealized fault**:
  - fault decreases Young's modulus of stacked system
- Effect of **rough** fracture and fracture-filling **viscous fluid**:
  - fracture roughness decreases stiffness of the the fractured system
  - apparent elastic moduli are highly increased possibly due to heterogeneous deformation of the plates
  - compaction/shearing of viscous fluid contributes to system stiffness



- Data processing of ultrasonic measurements
  - characterize fault state by calculating transmission and reflection coefficients and their dependence on incident angle
- Displacement transducer
  - calibration during cyclic displacement to correct for hysteresis
- Numerical modeling
  - quasi-static finite-element simulations of fluid-filled fractures
  - comparison between model and experimental results

Fractured rock



Numerical model

